Energy density functional methods for nuclear structure and neutrinoless double beta decay

Tomás R. Rodríguez

NAVI/JINA Collaboration-Meeting 2012

MSU November 2012

Bundesministerium für Bildung und Forschung

HIC for FAIR Helmholtz International Center

NAVI Nuclear Astrophysics Virtual Institute

TECHNISCHE UNIVERSITÄT DARMSTADT

Outline

1. Introduction

2. Nuclear structure

3. Neutrinoless double beta decay

4. Summary and outlook

Motivation

Description of the nuclear structure valid for the whole nuclear chart with a single effective interaction.

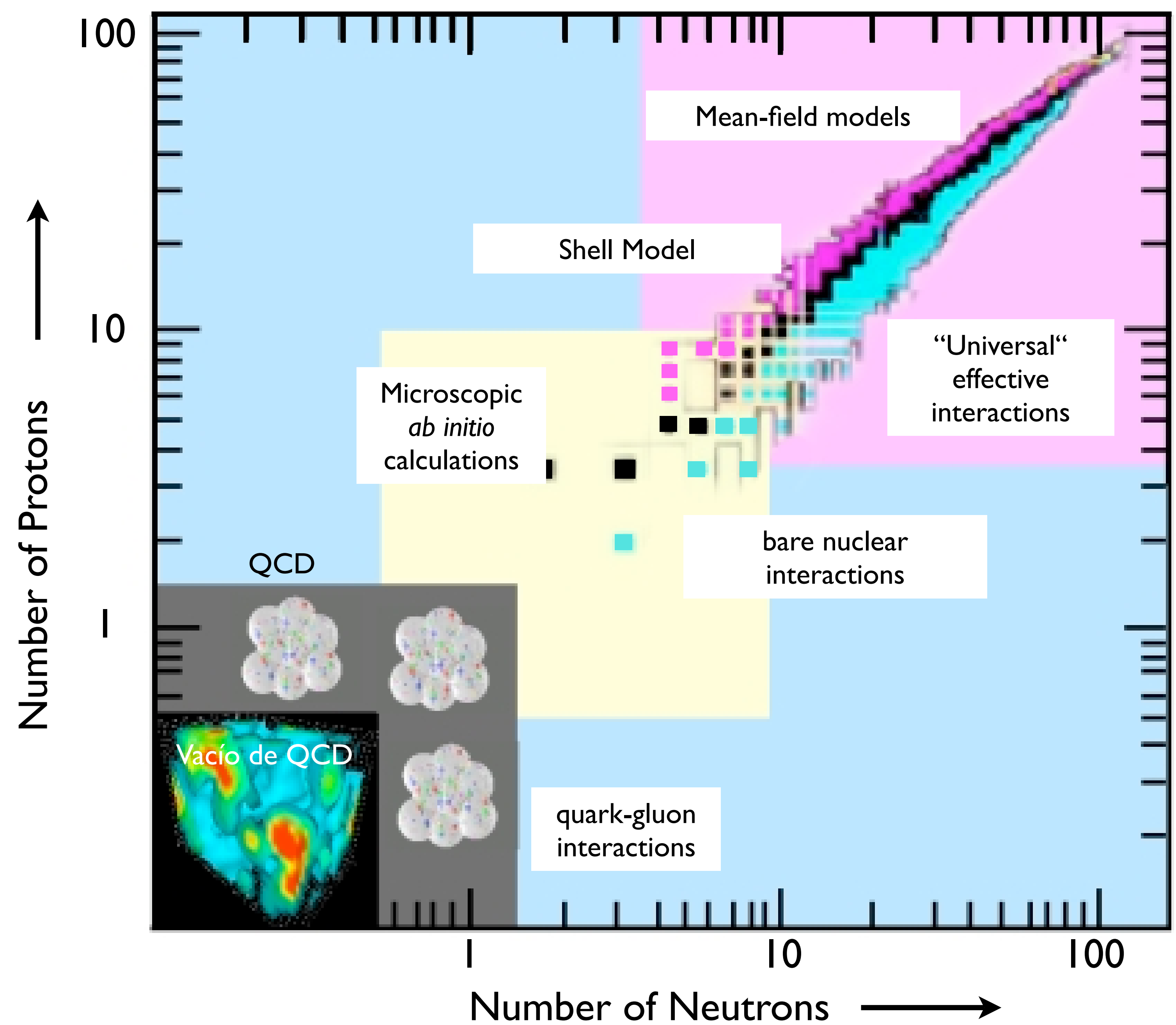

Description of the nuclear structure valid for the whole nuclear chart with a single effective interaction.

- Skyrme functionals

- Gogny functionals

- Relativistic functionals

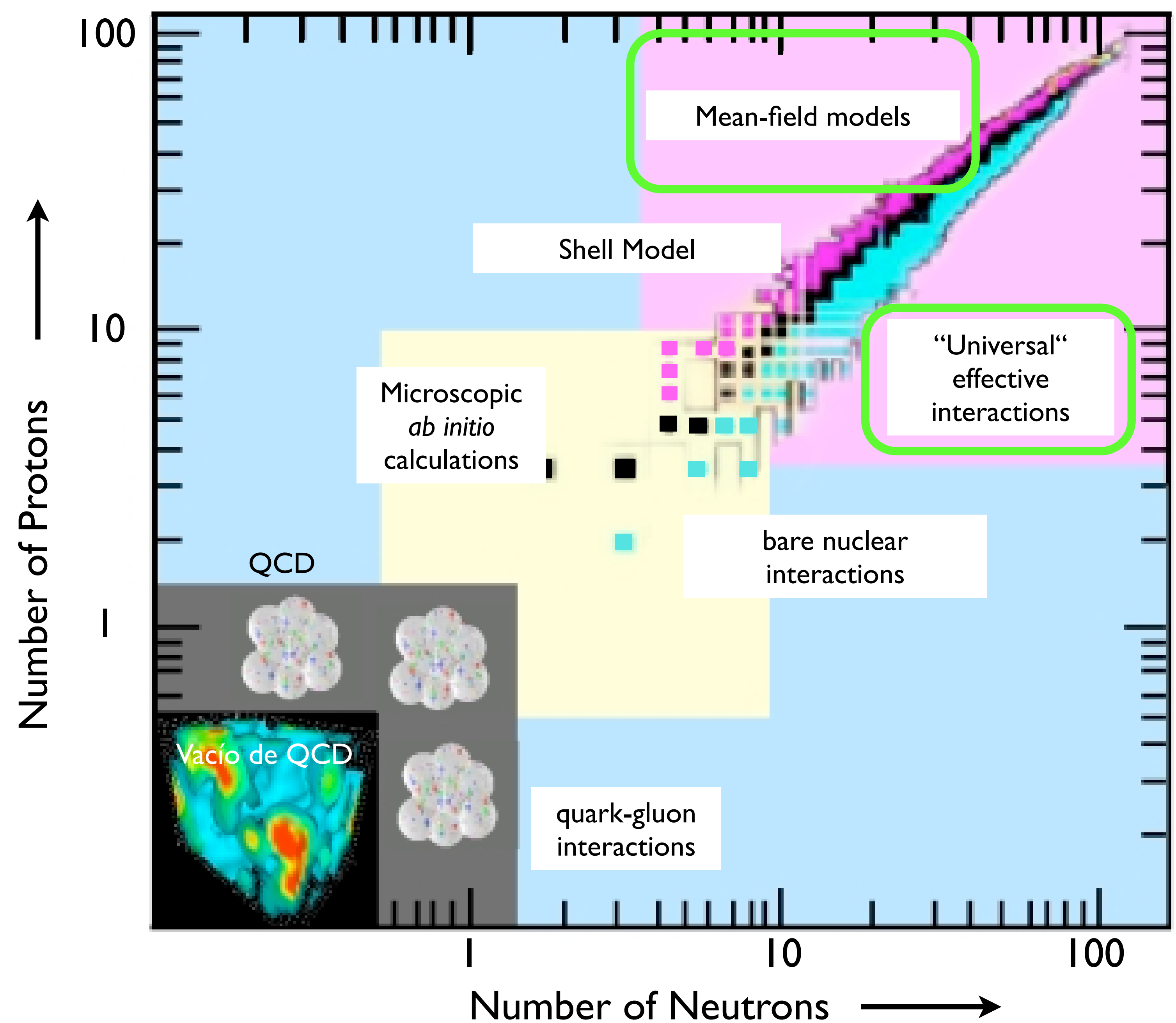

Theoretical framework

- **Effective nucleon-nucleon interaction:**

Gogny force (D1S-D1M) that is able to describe properly many phenomena along the whole nuclear chart.

$$V(1,2) = \sum_{i=1}^{2} e^{-(\vec{r}_1-\vec{r}_2)^2/\mu_i^2} \left(W_i + B_i P^\sigma - H_i P^\tau - M_i P^\sigma P^\tau\right)$$

$$+iW_0(\sigma_1+\sigma_2)\vec{k}\times\delta(\vec{r}_1-\vec{r}_2)\vec{k} + t_3(1+x_0P^\sigma)\delta(\vec{r}_1-\vec{r}_2)\rho^\alpha\left((\vec{r}_1+\vec{r}_2)/2\right)$$

$$+V_{\mathrm{Coulomb}}(\vec{r}_1,\vec{r}_2)$$

Theoretical framework

- **Effective nucleon-nucleon interaction:**

Gogny force (D1S-D1M) that is able to describe properly many phenomena along the whole nuclear chart.

$$V(1,2)=\sum_{i=1}^{2}e^{-(\vec{r}_1-\vec{r}_2)^2/\mu_i^2}\left(W_i+B_iP^{\sigma}-H_iP^{\tau}-M_iP^{\sigma}P^{\tau}\right)$$

central term

$$+iW_0(\sigma_1+\sigma_2)\vec{k}\times\delta(\vec{r}_1-\vec{r}_2)\vec{k}+t_3(1+x_0P^{\sigma})\delta(\vec{r}_1-\vec{r}_2)\rho^{\alpha}\left((\vec{r}_1+\vec{r}_2)/2\right)$$

$$+V_{\mathrm{Coulomb}}(\vec{r}_1,\vec{r}_2)$$

Theoretical framework

- **Effective nucleon-nucleon interaction:**

Gogny force (D1S-D1M) that is able to describe properly many phenomena along the whole nuclear chart.

$$V(1,2)=\sum_{i=1}^{2}e^{-(\vec{r}_1-\vec{r}_2)^2/\mu_i^2}\left(W_i+B_iP^\sigma-H_iP^\tau-M_iP^\sigma P^\tau\right)$$

central term

$$+iW_0(\sigma_1+\sigma_2)\vec{k}\times\delta(\vec{r}_1-\vec{r}_2)\vec{k}+t_3(1+x_0P^\sigma)\delta(\vec{r}_1-\vec{r}_2)\rho^\alpha\left((\vec{r}_1+\vec{r}_2)/2\right)$$

spin-orbit term

$$+V_{\mathrm{Coulomb}}(\vec{r}_1,\vec{r}_2)$$

Theoretical framework

- **Effective nucleon-nucleon interaction:**

Gogny force (D1S-D1M) that is able to describe properly many phenomena along the whole nuclear chart.

$$V(1,2)=\sum_{i=1}^{2}e^{-(\vec{r}_1-\vec{r}_2)^2/\mu_i^2}\left(W_i+B_iP^\sigma-H_iP^\tau-M_iP^\sigma P^\tau\right)$$ central term

spin-orbit term

$$+iW_0(\sigma_1+\sigma_2)\vec{k}\times\delta(\vec{r}_1-\vec{r}_2)\vec{k}+t_3(1+x_0P^\sigma)\delta(\vec{r}_1-\vec{r}_2)\rho^\alpha\left((\vec{r}_1+\vec{r}_2)/2\right)$$

density-dependent term

$$+V_{\mathrm{Coulomb}}(\vec{r}_1,\vec{r}_2)$$

- **Effective nucleon-nucleon interaction:**

Gogny force (D1S-D1M) that is able to describe properly many phenomena along the whole nuclear chart.

$$V(1,2) = \sum_{i=1}^{2} e^{-(\vec{r}_1-\vec{r}_2)^2/\mu_i^2}\left(W_i + B_i P^{\sigma} - H_i P^{\tau} - M_i P^{\sigma} P^{\tau}\right)$$

central term

$$+ iW_0(\sigma_1+\sigma_2)\vec{k}\times\delta(\vec{r}_1-\vec{r}_2)\vec{k} + t_3(1+x_0P^{\sigma})\delta(\vec{r}_1-\vec{r}_2)\rho^{\alpha}\left((\vec{r}_1+\vec{r}_2)/2\right)$$

spin-orbit term

density-dependent term

$$+V_{\mathrm{Coulomb}}(\vec{r}_1,\vec{r}_2)$$

Coulomb term

- **Effective nucleon-nucleon interaction:**

Gogny force (D1S-D1M) that is able to describe properly many phenomena along the whole nuclear chart.

$$V(1,2)=\sum_{i=1}^{2}e^{-(\vec{r}_1-\vec{r}_2)^2/\mu_i^2}\left(W_i+B_iP^\sigma-H_iP^\tau-M_iP^\sigma P^\tau\right)$$ central term

spin-orbit term
$$+iW_0(\sigma_1+\sigma_2)\vec{k}\times\delta(\vec{r}_1-\vec{r}_2)\vec{k}+t_3(1+x_0P^\sigma)\delta(\vec{r}_1-\vec{r}_2)\rho^\alpha\left((\vec{r}_1+\vec{r}_2)/2\right)$$
density-dependent term

$$+V_{\mathrm{Coulomb}}(\vec{r}_1,\vec{r}_2)$$ Coulomb term

- **Method of solving the many-body problem:**

Theoretical framework

- **Effective nucleon-nucleon interaction:**

Gogny force (D1S-D1M) that is able to describe properly many phenomena along the whole nuclear chart.

$$V(1,2)=\sum_{i=1}^{2}e^{-(\vec{r}_1-\vec{r}_2)^2/\mu_i^2}\left(W_i+B_iP^\sigma-H_iP^\tau-M_iP^\sigma P^\tau\right)$$ central term

$$+iW_0(\sigma_1+\sigma_2)\vec{k}\times\delta(\vec{r}_1-\vec{r}_2)\vec{k}+t_3(1+x_0P^\sigma)\delta(\vec{r}_1-\vec{r}_2)\rho^\alpha\left((\vec{r}_1+\vec{r}_2)/2\right)$$

spin-orbit term; density-dependent term

$$+V_{\text{Coulomb}}(\vec{r}_1,\vec{r}_2)$$ Coulomb term

- **Method of solving the many-body problem:**

First step: Particle Number Projection (before the variation) of HFB-type wave functions.

- **Effective nucleon-nucleon interaction:**

Gogny force (D1S-D1M) that is able to describe properly many phenomena along the whole nuclear chart.

$$V(1,2) = \sum_{i=1}^{2} e^{-(\vec{r}_1-\vec{r}_2)^2/\mu_i^2}\left(W_i + B_i P^{\sigma} - H_i P^{\tau} - M_i P^{\sigma} P^{\tau}\right)$$ central term

$$+iW_0(\sigma_1+\sigma_2)\vec{k}\times\delta(\vec{r}_1-\vec{r}_2)\vec{k} + t_3(1+x_0 P^{\sigma})\delta(\vec{r}_1-\vec{r}_2)\rho^{\alpha}\left((\vec{r}_1+\vec{r}_2)/2\right)$$

spin-orbit term; density-dependent term

$$+V_{\mathrm{Coulomb}}(\vec{r}_1,\vec{r}_2)$$ Coulomb term

- **Method of solving the many-body problem:**

First step: Particle Number Projection (before the variation) of HFB-type wave functions.

Second step: Simultaneous **Particle Number and Angular Momentum Projection** (after the variation).

- **Effective nucleon-nucleon interaction:**

Gogny force (D1S-D1M) that is able to describe properly many phenomena along the whole nuclear chart.

$$V(1,2) = \sum_{i=1}^{2} e^{-(\vec{r}_1-\vec{r}_2)^2/\mu_i^2}\left(W_i + B_i P^\sigma - H_i P^\tau - M_i P^\sigma P^\tau\right)$$ central term

$$+iW_0(\sigma_1+\sigma_2)\vec{k}\times\delta(\vec{r}_1-\vec{r}_2)\vec{k} + t_3(1+x_0P^\sigma)\delta(\vec{r}_1-\vec{r}_2)\rho^\alpha\left((\vec{r}_1+\vec{r}_2)/2\right)$$

spin-orbit term; density-dependent term

$$+V_{\text{Coulomb}}(\vec{r}_1,\vec{r}_2)$$ Coulomb term

- **Method of solving the many-body problem:**

First step: Particle Number Projection (before the variation) of HFB-type wave functions.

Second step: Simultaneous **Particle Number and Angular Momentum Projection** (after the variation).

Third step: Configuration mixing within the framework of the **Generator Coordinate Method (GCM)**.

Axial calculations ^{24}Mg

$$|\Phi(\beta)\rangle$$ product-type many body wave function

$$|\Phi^{N,Z}(\beta)\rangle = \hat{P}^N \hat{P}^Z |\Phi(\beta)\rangle$$

$$E^{N,Z}(\beta)$$ Potential Energy Surface

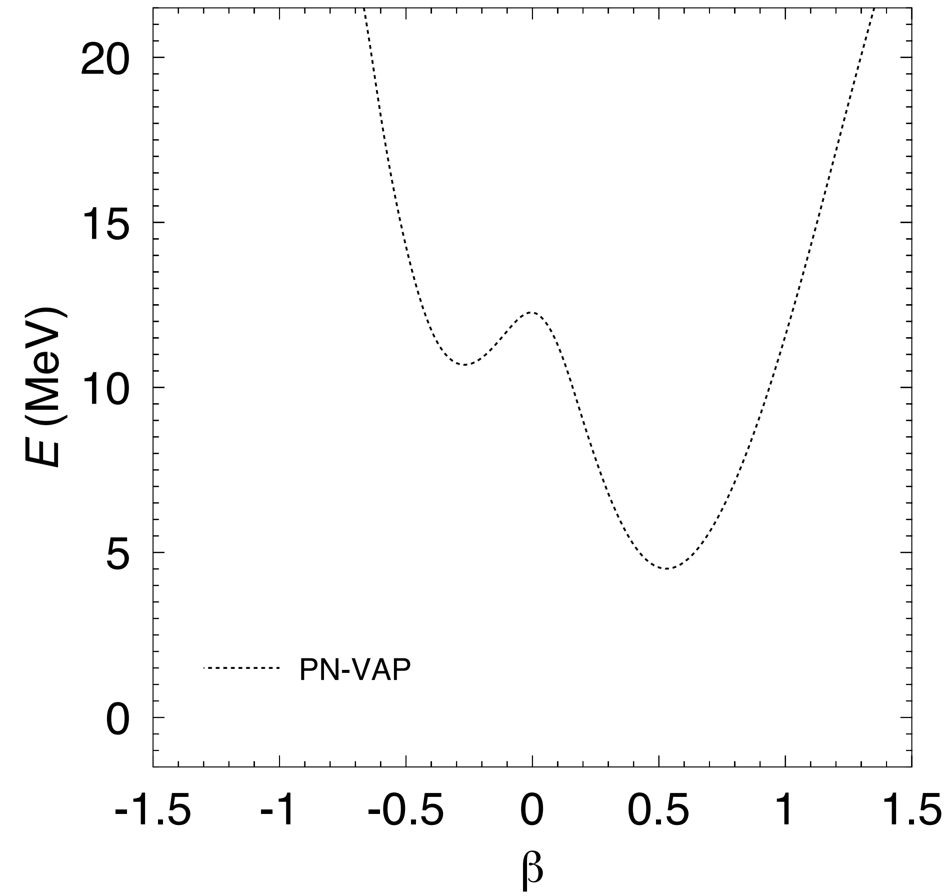

Axial calculations ^{24}Mg

$$|\Phi(\beta)\rangle$$ product-type many body wave function

$$|\Phi^{N,Z}(\beta)\rangle = \hat{P}^N \hat{P}^Z |\Phi(\beta)\rangle$$

$$E^{N,Z}(\beta)$$ Potential Energy Surface

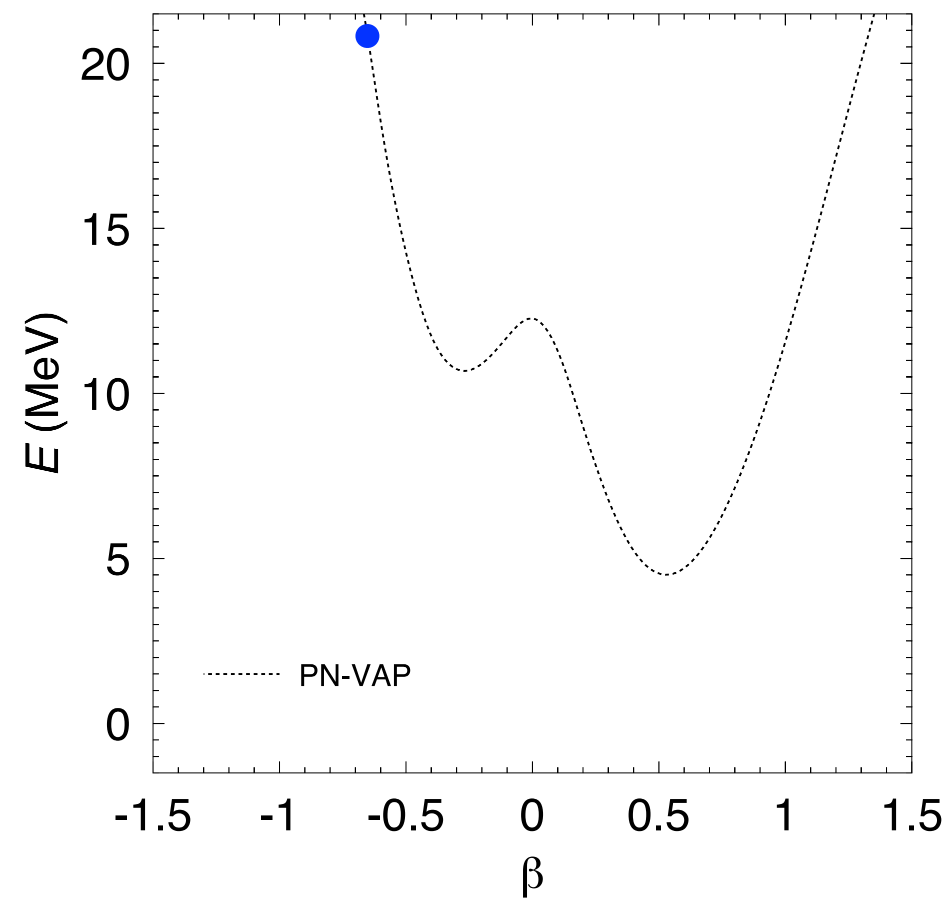

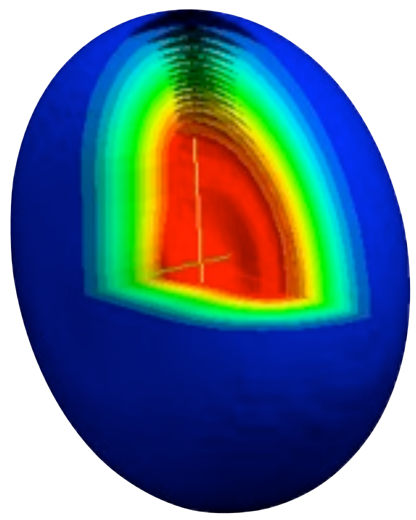

Particle number and angular momentum projection

Axial calculations ^{24}Mg

$$|\Phi(\beta)\rangle$$

product-type many body wave function

$$|\Phi^{I,M;N,Z}(\beta)\rangle = \hat{P}^I_{00}\hat{P}^N\hat{P}^Z|\Phi(\beta)\rangle$$

$$E^{I,N,Z}(\beta)$$

Projected Potential Energy Surface

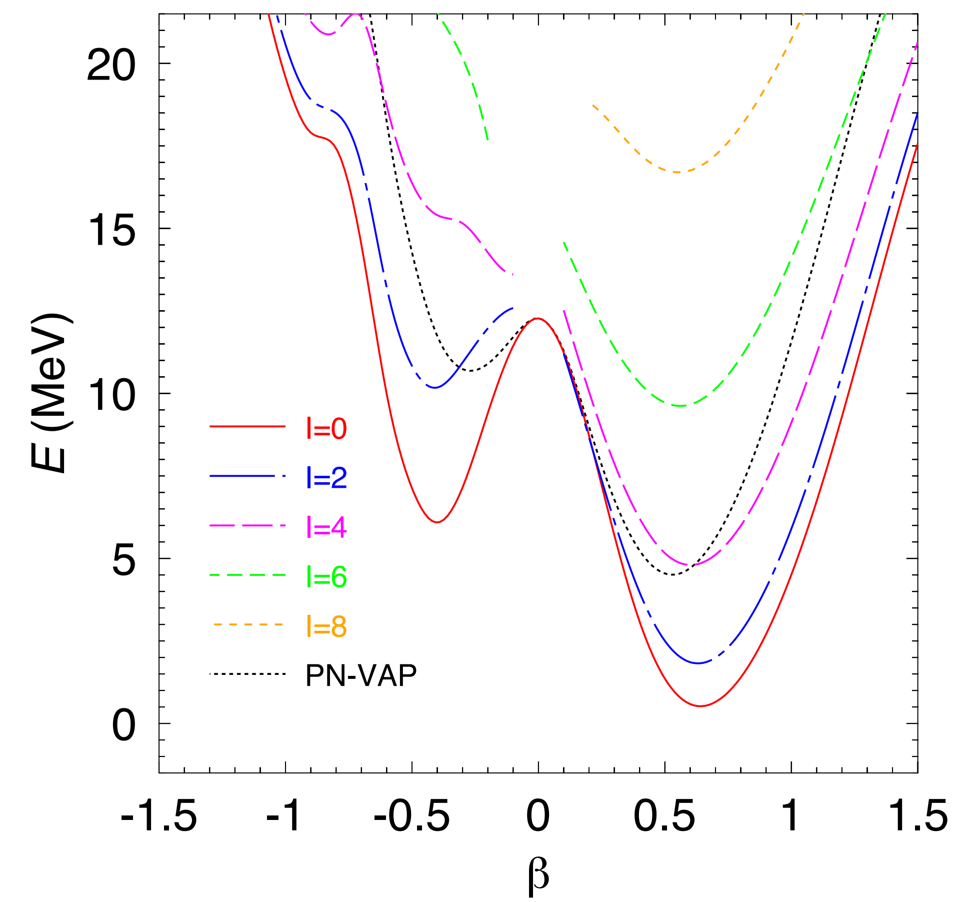

Configuration (shape) mixing

Axial calculations ^{24}Mg

Configuration mixing within the framework of the **Generator Coordinate Method (GCM)**.

$$|\Psi^{I;N,Z;\sigma}\rangle = \sum_{\beta} f^{I;N,Z;\sigma}(\beta)\hat{P}^{I}_{00}\hat{P}^{N}\hat{P}^{Z}|\Phi(\beta)\rangle$$

Configuration mixing

$$\sum_{\beta'}\left(\mathcal{H}^{I;NZ}_{\beta\beta'} - E^{I;NZ;\sigma}\mathcal{N}^{I;NZ}_{\beta\beta'}\right) f^{I;NZ;\sigma}_{\beta'} = 0$$

$$\mathcal{N}^{I;NZ}_{\beta\beta'} \equiv \langle\Phi(\beta)|P^{I}_{00}P^{N}P^{Z}|\Phi(\beta')\rangle$$

$$\mathcal{H}^{I;NZ}_{\beta\beta'} \equiv \langle\Phi(\beta)|\hat{H}_{2b}P^{I}_{00}P^{N}P^{Z}|\Phi(\beta')\rangle + \varepsilon^{I;NZ}_{DD}\left[\Phi(\beta),\Phi'(\beta')\right]$$

Hill-Wheeler-Griffin equations

- **Energy spectrum**
- **Observables (mass, radius, B(E2), etc.)**
- **“Collective w.f.”**

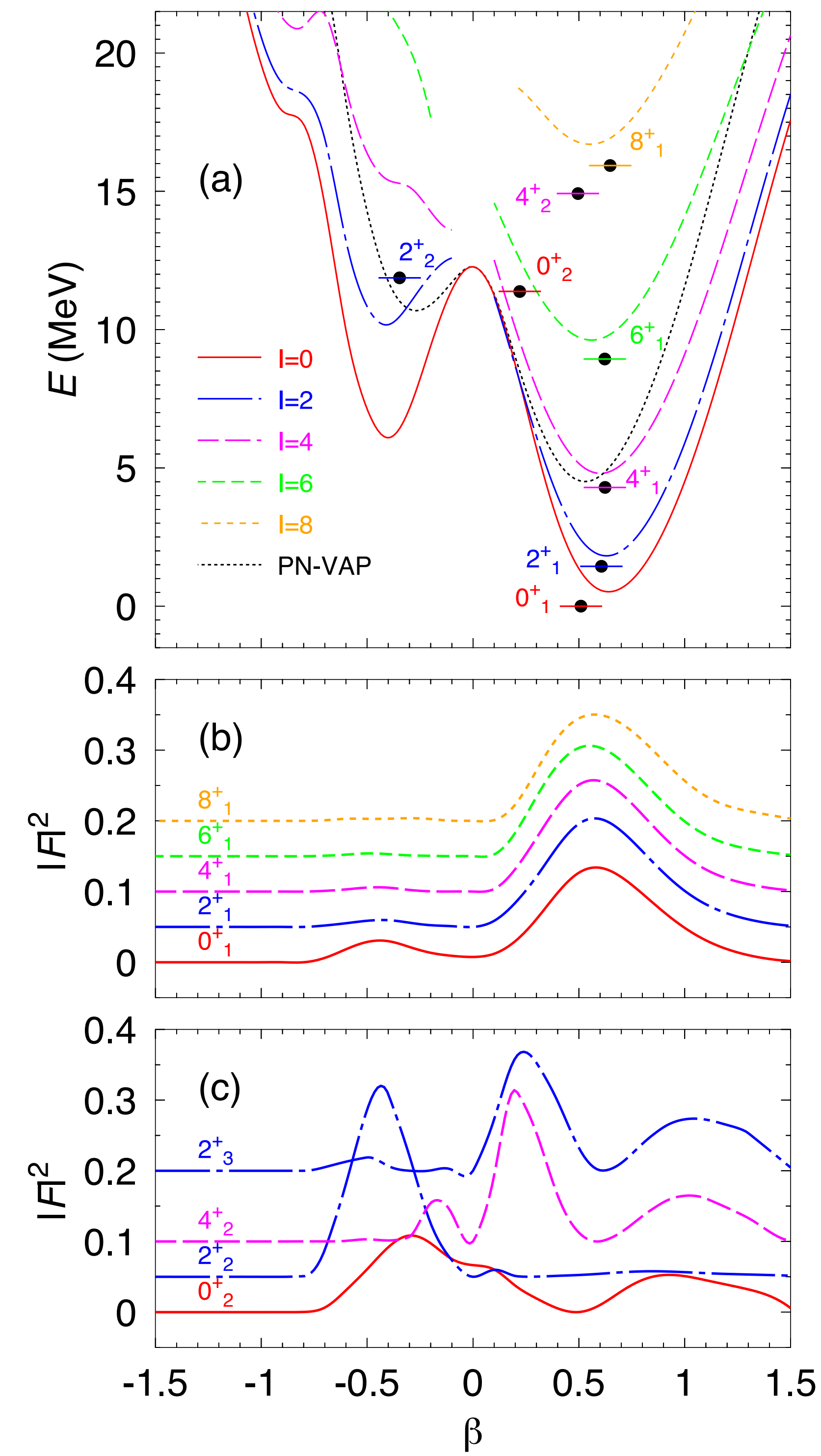

Triaxial calculations ^{24}Mg

$$\delta E^{N,Z}\left[\bar{\Phi}(\beta,\gamma)\right]\Big|_{\bar{\Phi}=\Phi}=0 \qquad E^{N,Z}[\Phi]=\frac{\langle\Phi|\hat{H}_{2b}\hat{P}^{N}\hat{P}^{Z}|\Phi\rangle}{\langle\Phi|\hat{P}^{N}\hat{P}^{Z}|\Phi\rangle}+\varepsilon_{DD}^{N,Z}(\Phi)-\lambda_{q_{20}}\langle\Phi|\hat{Q}_{20}|\Phi\rangle-\lambda_{q_{22}}\langle\Phi|\hat{Q}_{22}|\Phi\rangle$$

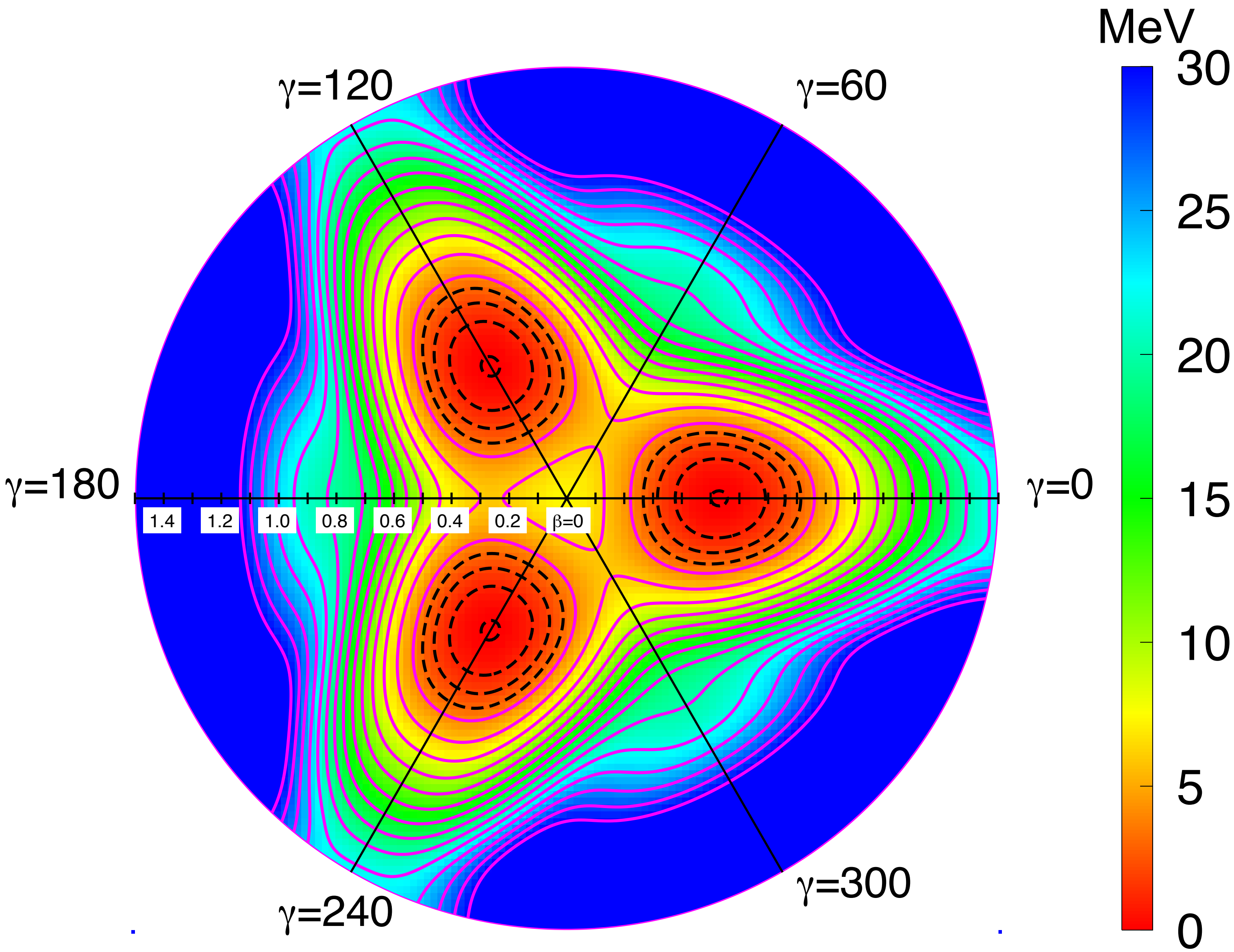

- Symmetry corresponding to the different orientation of the axes
- All configurations are included between γ∈[0º,60º]

Triaxial calculations ^{24}Mg

$$\delta E^{N,Z}\left[\bar{\Phi}(\beta,\gamma)\right]\Big|_{\bar{\Phi}=\Phi}=0 \qquad E^{N,Z}[\Phi]=\frac{\langle\Phi|\hat{H}_{2b}\hat{P}^{N}\hat{P}^{Z}|\Phi\rangle}{\langle\Phi|\hat{P}^{N}\hat{P}^{Z}|\Phi\rangle}+\varepsilon_{DD}^{N,Z}(\Phi)-\lambda_{q_{20}}\langle\Phi|\hat{Q}_{20}|\Phi\rangle-\lambda_{q_{22}}\langle\Phi|\hat{Q}_{22}|\Phi\rangle$$

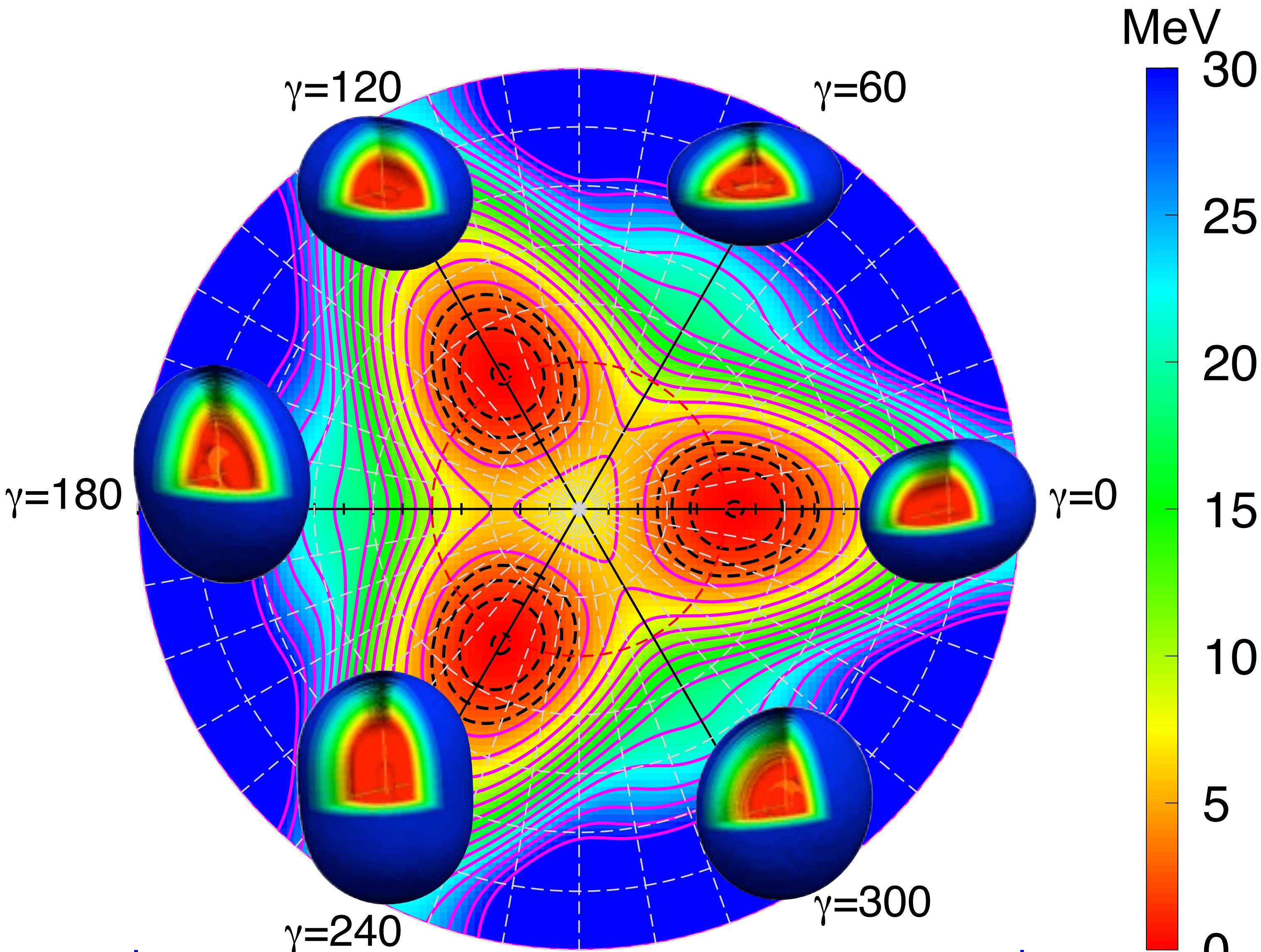

- Symmetry corresponding to the different orientation of the axes
- All configurations are included between γ∈[0º,60º]

Triaxial calculations ^{24}Mg

$$\delta E^{N,Z}\left[\bar{\Phi}(\beta,\gamma)\right]\Big|_{\bar{\Phi}=\Phi}=0 \qquad E^{N,Z}[\Phi]=\frac{\langle\Phi|\hat{H}_{2b}\hat{P}^N\hat{P}^Z|\Phi\rangle}{\langle\Phi|\hat{P}^N\hat{P}^Z|\Phi\rangle}+\varepsilon_{DD}^{N,Z}(\Phi)-\lambda_{q_{20}}\langle\Phi|\hat{Q}_{20}|\Phi\rangle-\lambda_{q_{22}}\langle\Phi|\hat{Q}_{22}|\Phi\rangle$$

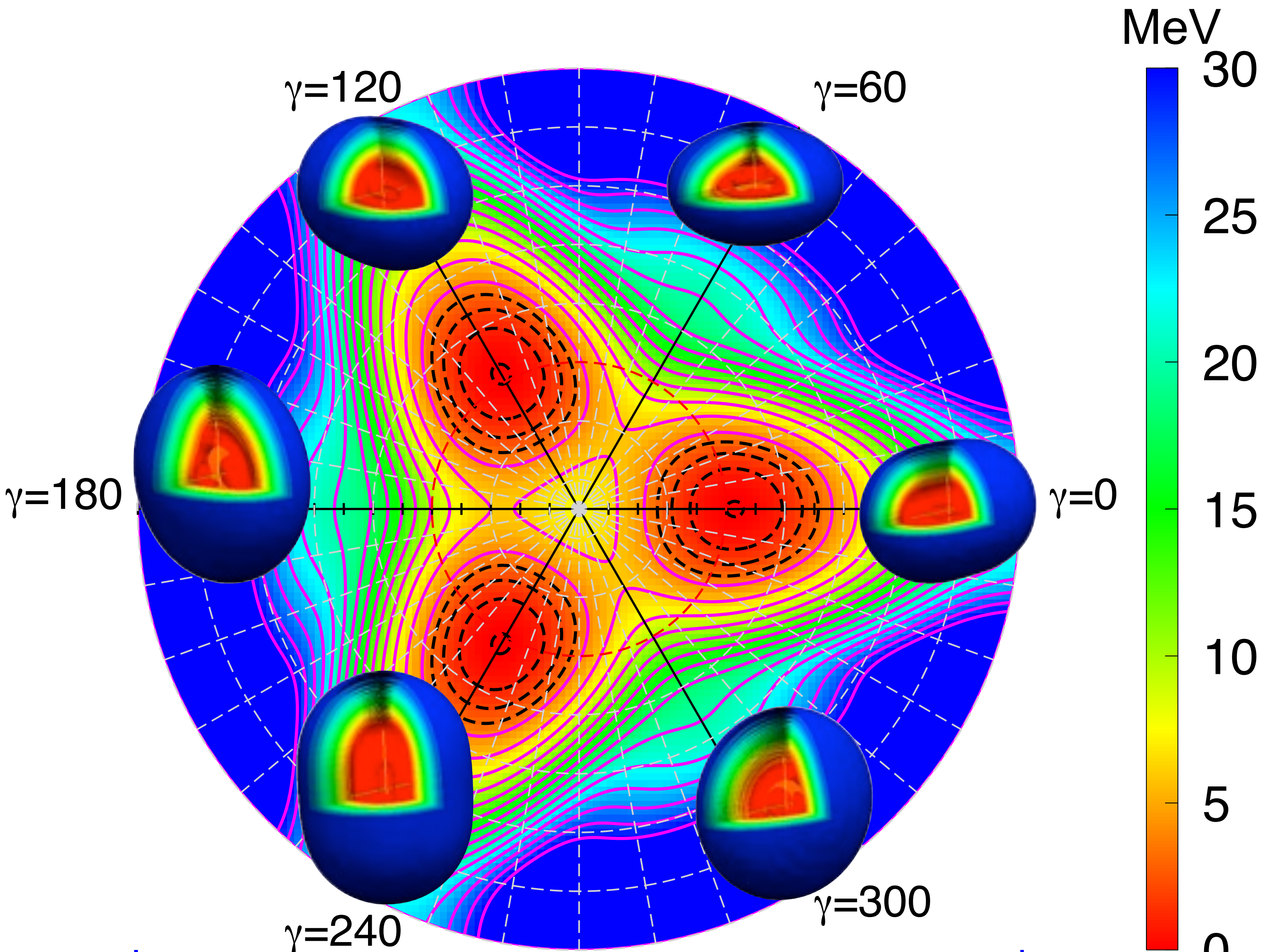

- Symmetry corresponding to the different orientation of the axes
- All configurations are included between γ∈[0º,60º]

Triaxial calculations ^{24}Mg

$$\delta E^{N,Z}\left[\bar{\Phi}(\beta,\gamma)\right]\Big|_{\bar{\Phi}=\Phi}=0 \qquad E^{N,Z}[\Phi]=\frac{\langle\Phi|\hat{H}_{2b}\hat{P}^{N}\hat{P}^{Z}|\Phi\rangle}{\langle\Phi|\hat{P}^{N}\hat{P}^{Z}|\Phi\rangle}+\varepsilon_{DD}^{N,Z}(\Phi)-\lambda_{q_{20}}\langle\Phi|\hat{Q}_{20}|\Phi\rangle-\lambda_{q_{22}}\langle\Phi|\hat{Q}_{22}|\Phi\rangle$$

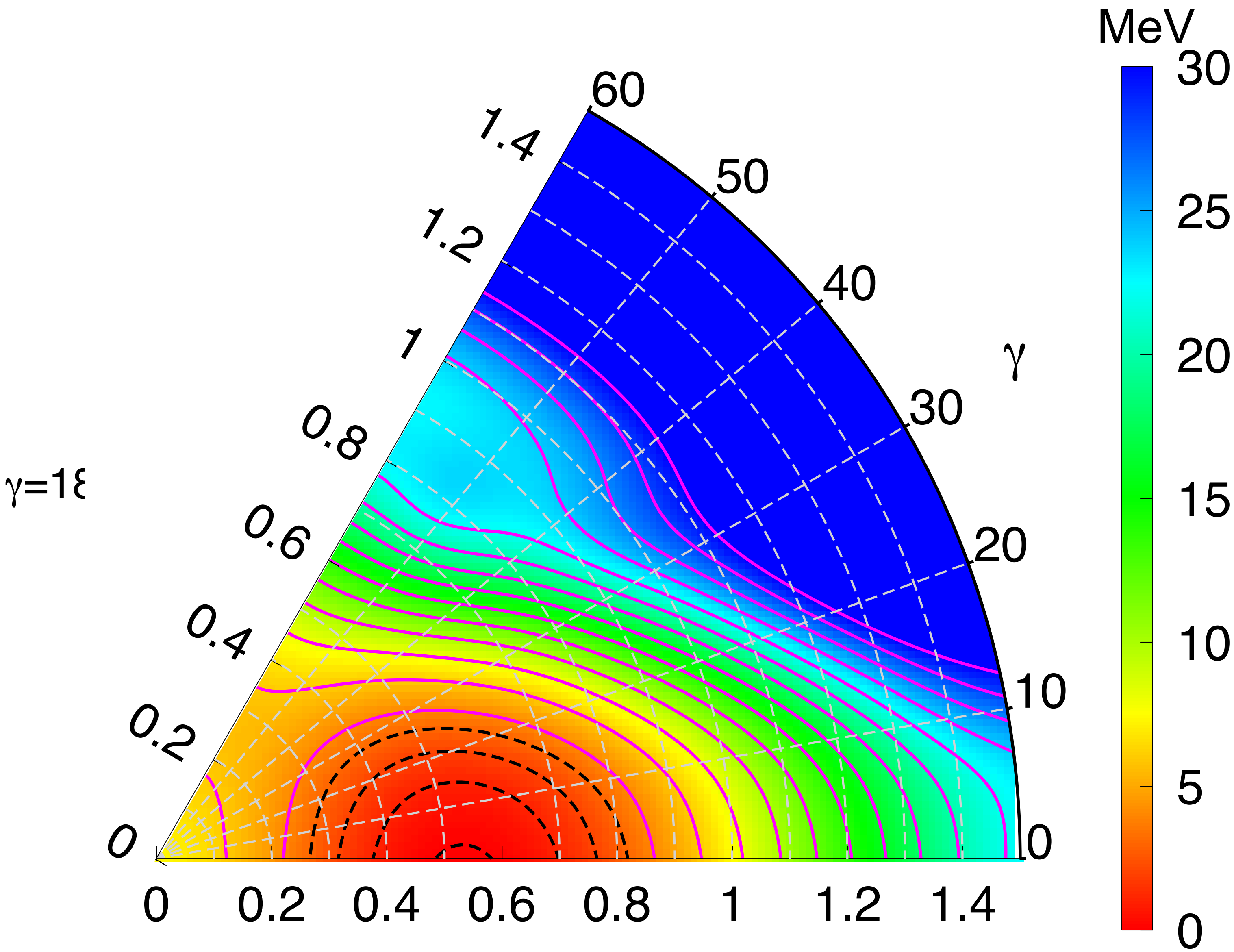

- Symmetry corresponding to the different orientation of the axes
- All configurations are included between γ∈[0º,60º]

Triaxial calculations ^{24}Mg

$$|IMK;NZ;\beta\gamma\rangle = \frac{2I+1}{8\pi^2}\int \mathcal{D}^{I*}_{MK}(\Omega)\hat{R}(\Omega)\hat{P}^N\hat{P}^Z|\Phi(\beta,\gamma)\rangle d\Omega$$

$$|IM;NZ;\beta\gamma\rangle = \sum_K g_K^{IM;NZ;\beta\gamma}|IMK;NZ;\beta\gamma\rangle$$

- Minimum displaced to triaxial shapes.

- Projection onto odd *I* angular momentum

- Softening of PES with increasing *I*.

- Difference between triaxial minimum and axial saddle point of ~ 0.7 MeV (0^+)

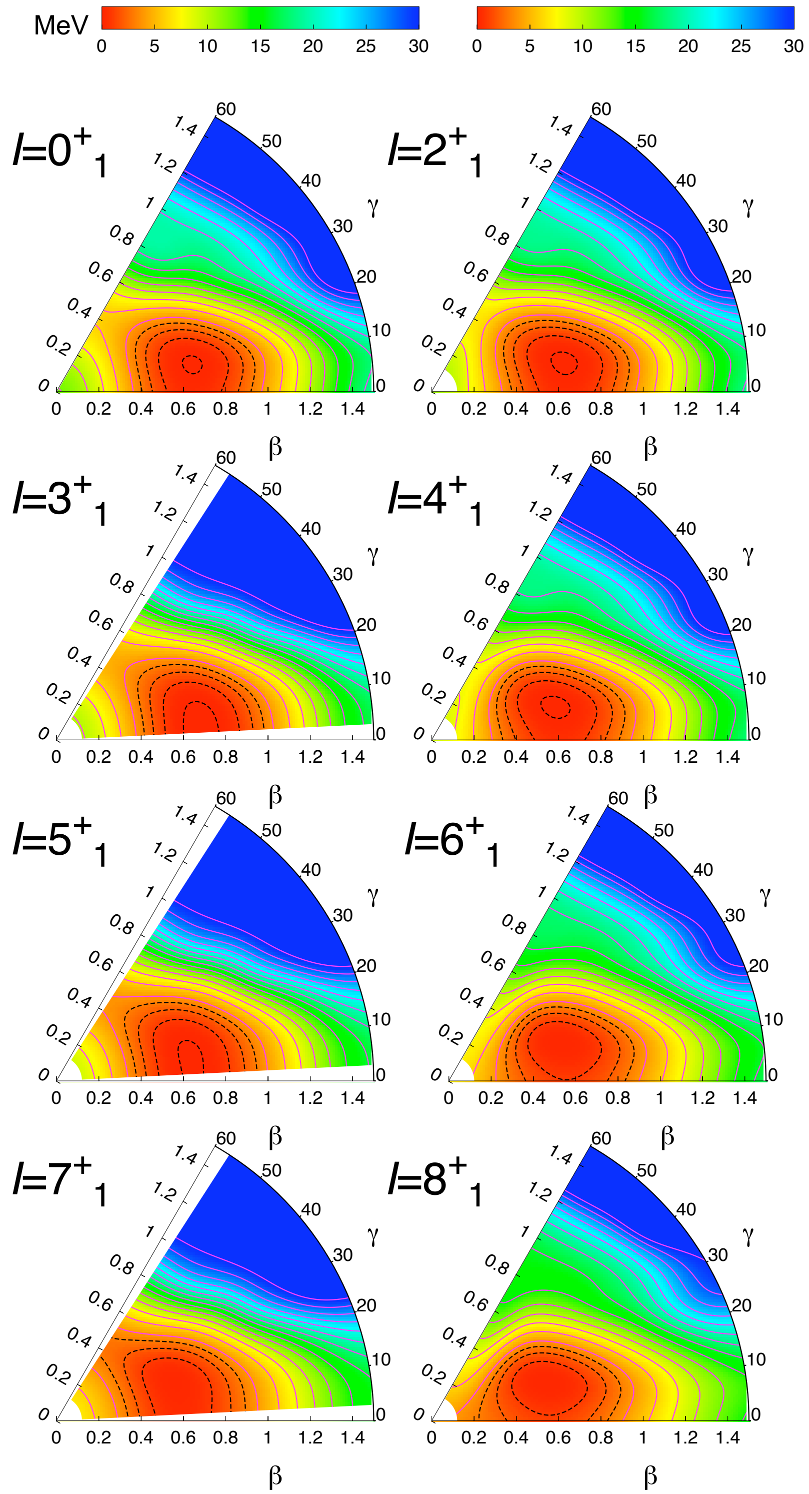

Triaxial calculations ^{24}Mg

Configuration mixing within the framework of the **Generator Coordinate Method (GCM).** ***K* and deformation mixing**

$$|IM;NZ\sigma\rangle = \sum_{K\beta\gamma} f^{I;NZ,\sigma}_{K\beta\gamma}|IMK;NZ;\beta\gamma\rangle$$

$$\sum_{K'\beta'\gamma'}\left(\mathcal{H}^{I;NZ}_{K\beta\gamma K'\beta'\gamma'} - E^{I;NZ;\sigma}\mathcal{N}^{I;NZ}_{K\beta\gamma K'\beta'\gamma'}\right) f^{I;NZ;\sigma}_{K'\beta'\gamma'} = 0$$

- Axial ground state rotational band

- Second band associated to a gamma band

-Third band with shape mixing

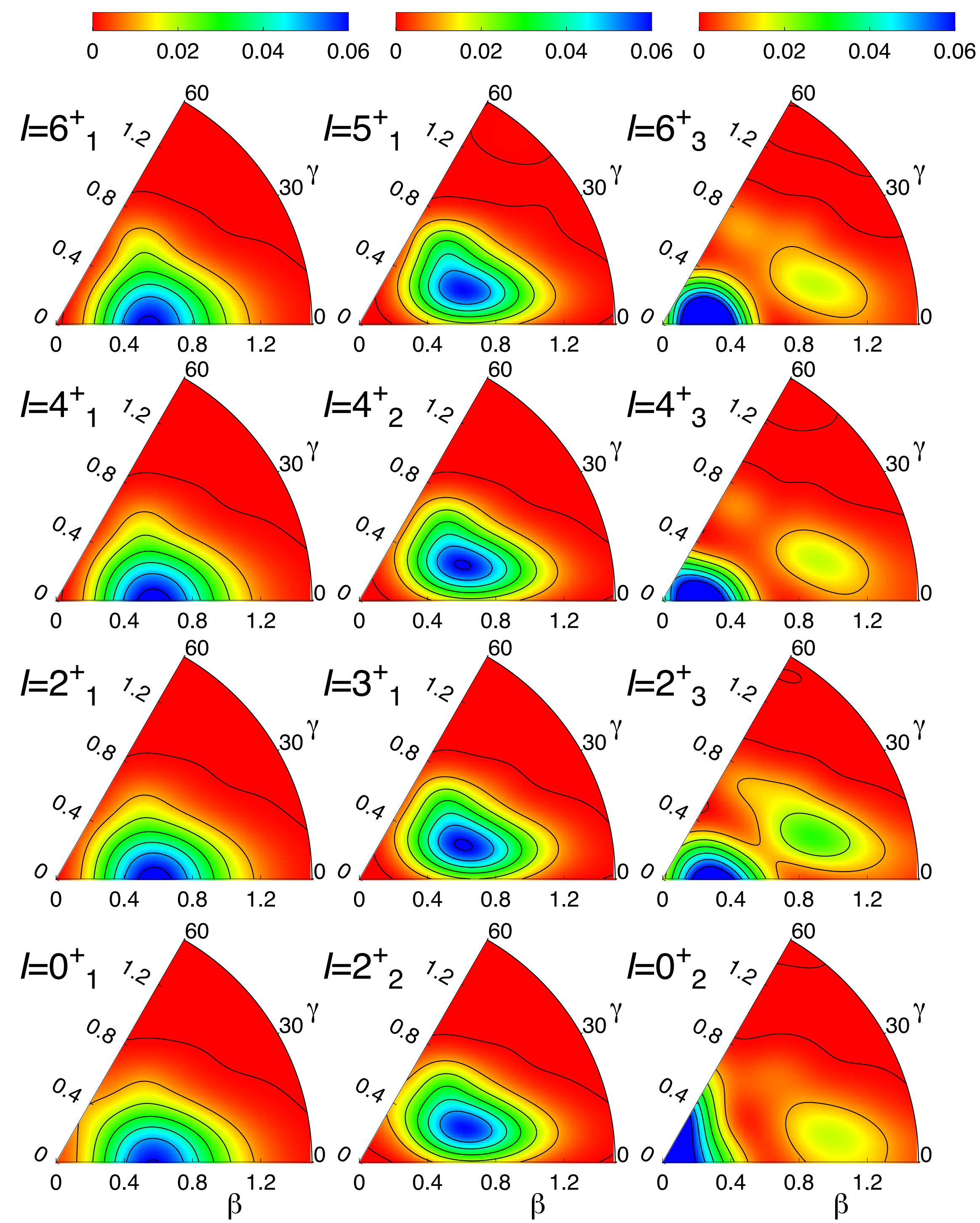

Configuration (shape) mixing

Triaxial calculations ^{24}Mg

Configuration mixing within the framework of the **Generator Coordinate Method (GCM)**.
***K* and deformation mixing**

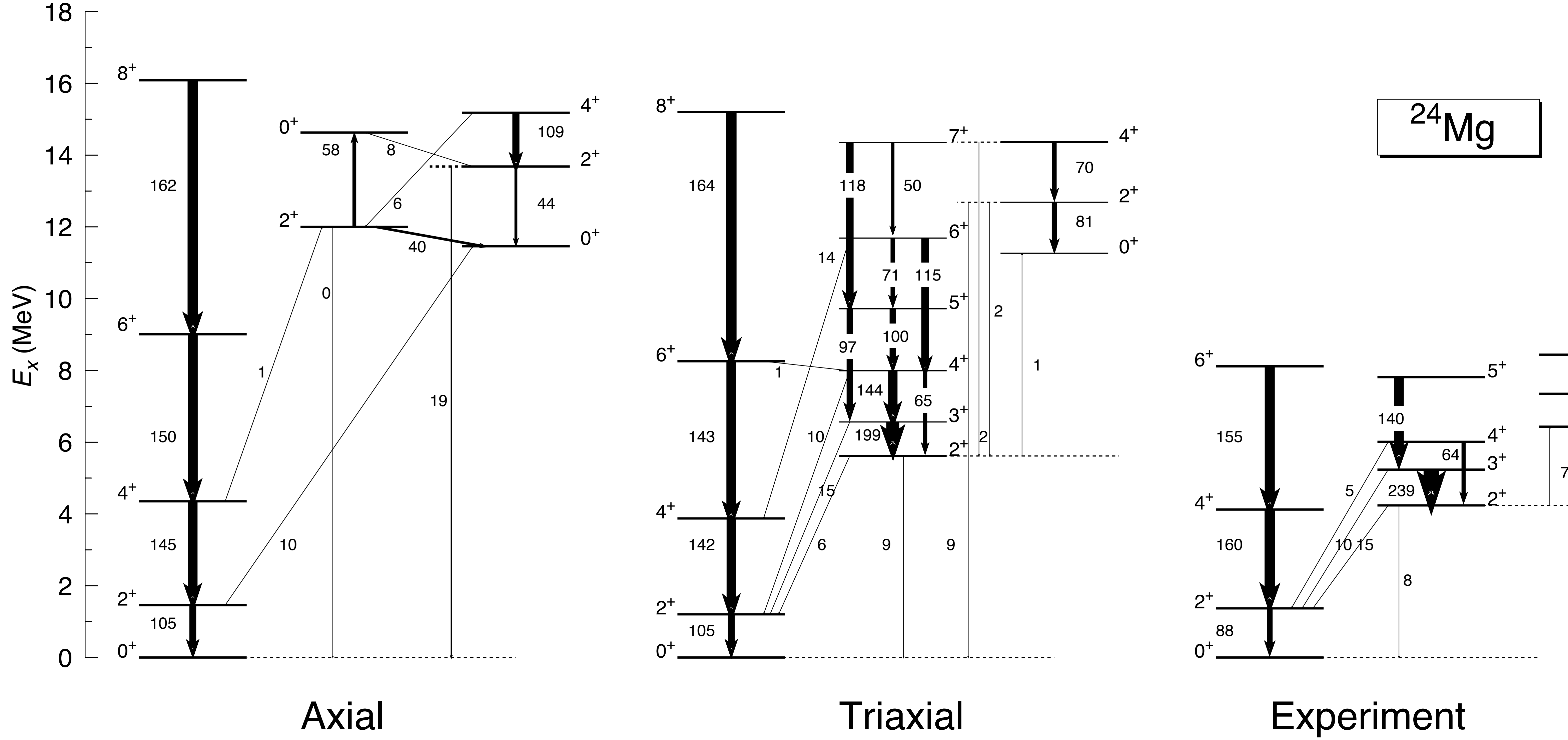

Shell closures

- Magic numbers in the valley of the stability

✓ Very stable (high binding energies per nucleon and separation energies).

✓ Spherical shape.

✓ High excitation energy of the first 2^+ state.

✓ Small reduced transition probabilities between the first 2^+ and ground states.

✓ Magic numbers (2, 8, 20, 28, 50, 82, 126) correspond to the shell closures of a harmonic oscillator+spin-orbit single particle potential.

- Magic numbers in exotic nuclei

✓ Degradation of the traditional shell closures: ^{32}Mg (N=20), ^{42}Si (N=28)

✓ Appearance of new shell closures: N=32

✓ Key relevance in r-process nucleosynthesis (waiting points)

✓ Shell quenching in N=82 for Cadmium isotopes?

Shell closures

- *N*=32 and/or *N*=34 in Ca, Ti and Cr isotopes.

The tendency of the **experimental data** for the excitation energies $E(2^+)$ and transition probabilities $B(E2,0^+\rightarrow 2^+)$ shows the presence of sub-shell closures.

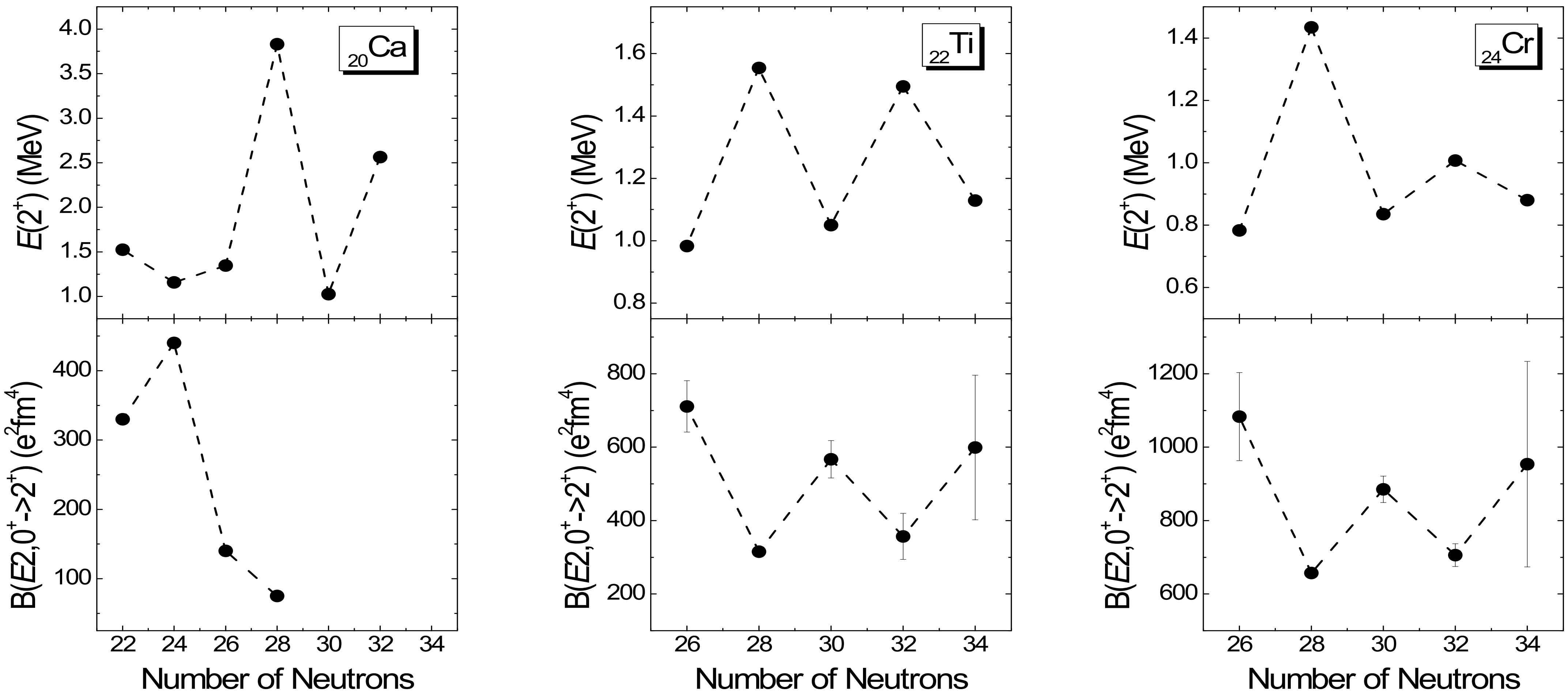

Schielke *et al* (PL B571, 29(2003)) Dinca *et al* (PR C71,041302(2005)) Bürger *et al* (PL B662, 29(2005))

Shell closures

- *N*=32 and/or *N*=34 in Ca, Ti and Cr isotopes.

The tendency of the **experimental data** for the excitation energies $E(2^+)$ and transition probabilities $B(E2,0^+\rightarrow 2^+)$ shows the presence of sub-shell closures.

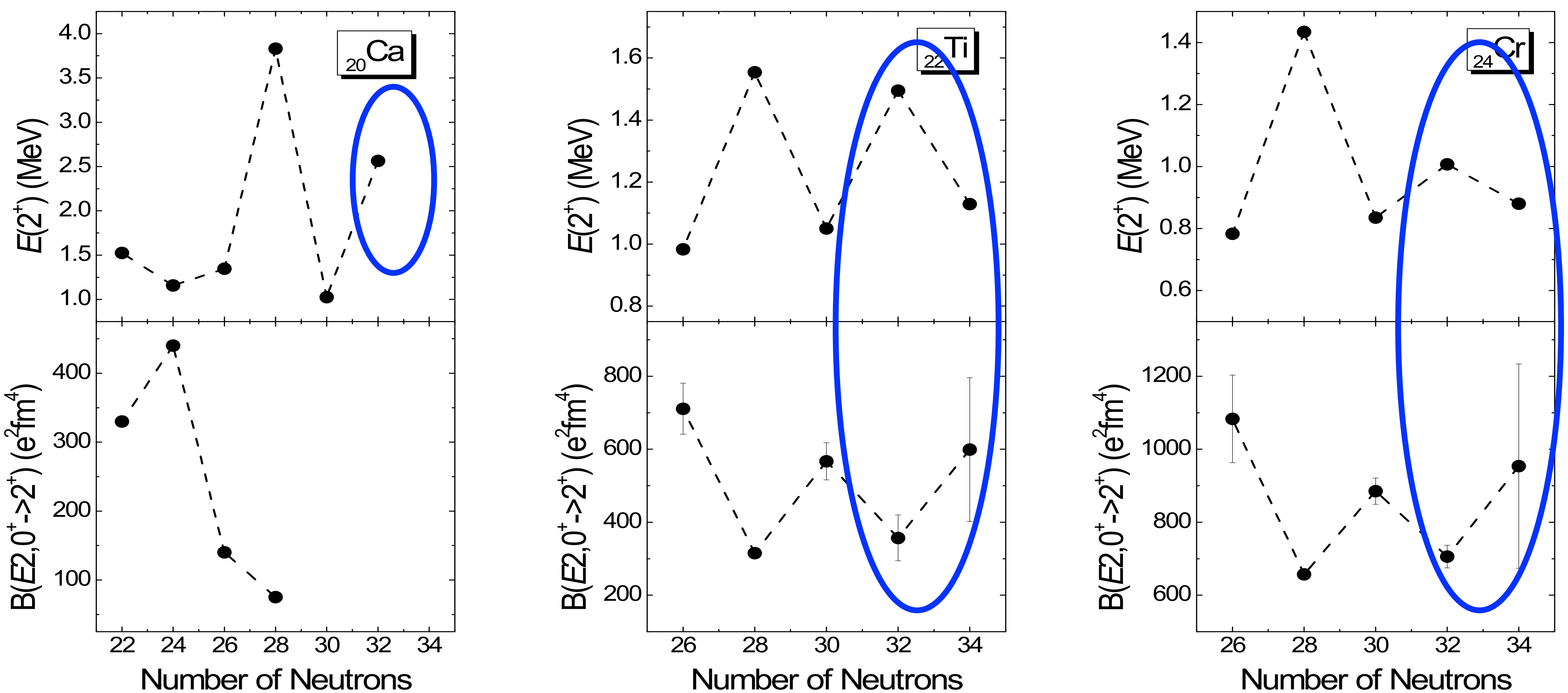

Schielke *et al* (PL B571, 29(2003)) Dinca *et al* (PR C71,041302(2005)) Bürger *et al* (PL B662, 29(2005))

Shell closures

- N=32 and/or N=34 in Ca, Ti and Cr isotopes.

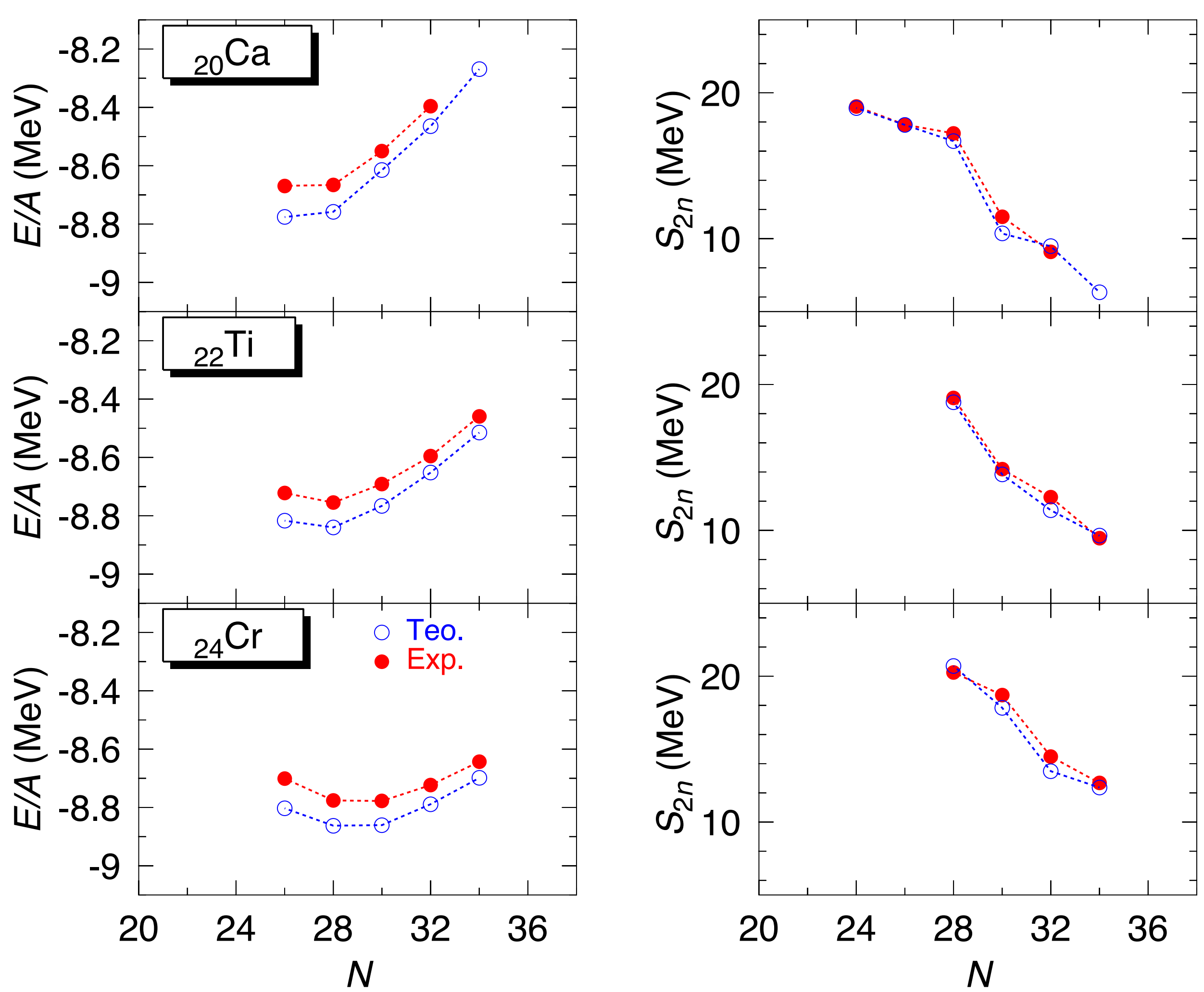

✓ AXIAL calculations

✓ Good agreement in the binding energies and two neutron separation energies.

T.R.R and J.L. Egido, Phys. Rev. Lett. 99, 062501 (2007)

• *N*=32 and/or *N*=34 in Ca, Ti and Cr isotopes.

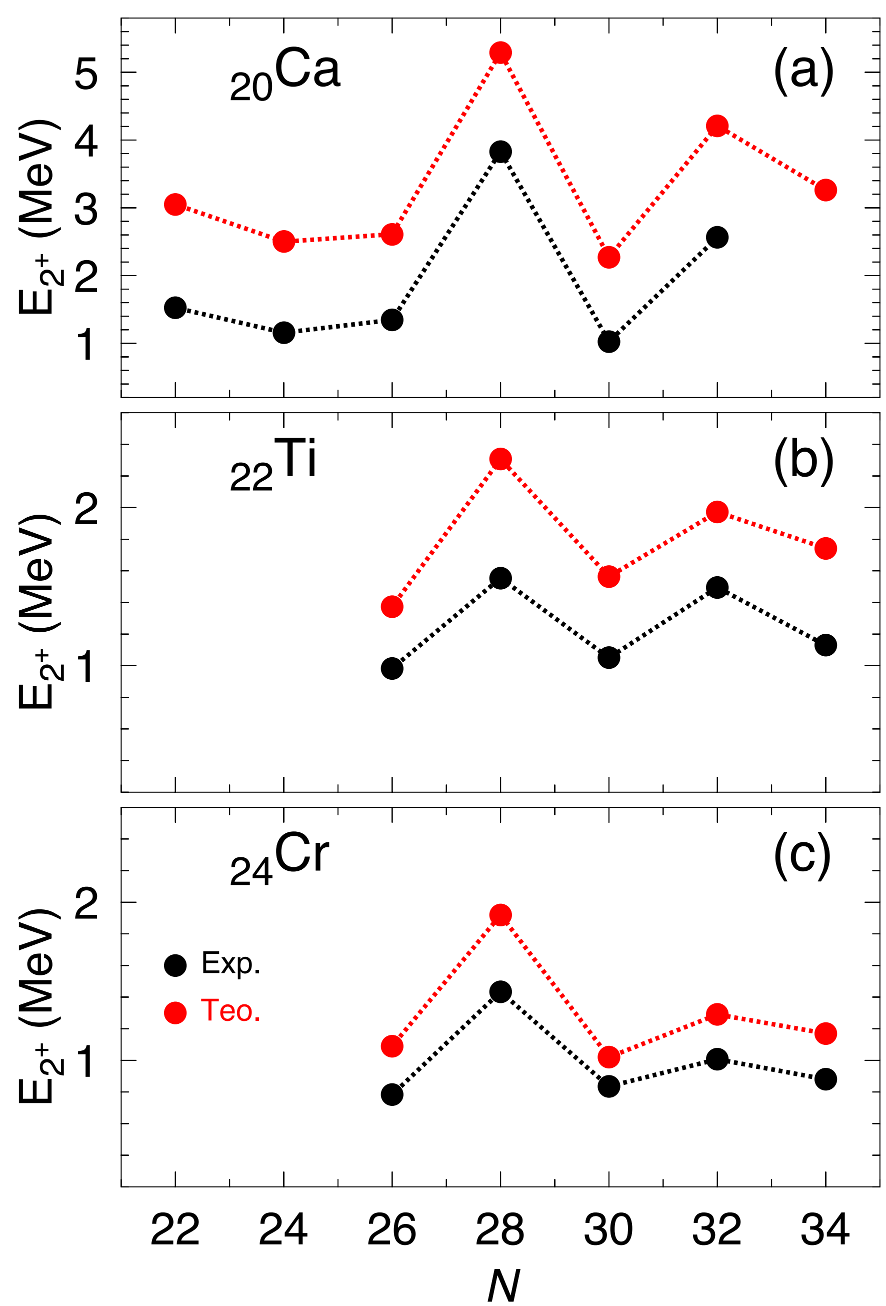

✓ AXIAL calculations

✓ Good agreement in the binding energies and two neutron separation energies.

✓ Excellent qualitative agreement for the excitation energies $E(2^+)$

✓ *N*=32 is a good sub-shell closure while *N*=34 is not.

T.R.R and J.L. Egido, Phys. Rev. Lett. 99, 06201 (2007)

- *N*=32 and/or *N*=34 in Ca, Ti and Cr isotopes.

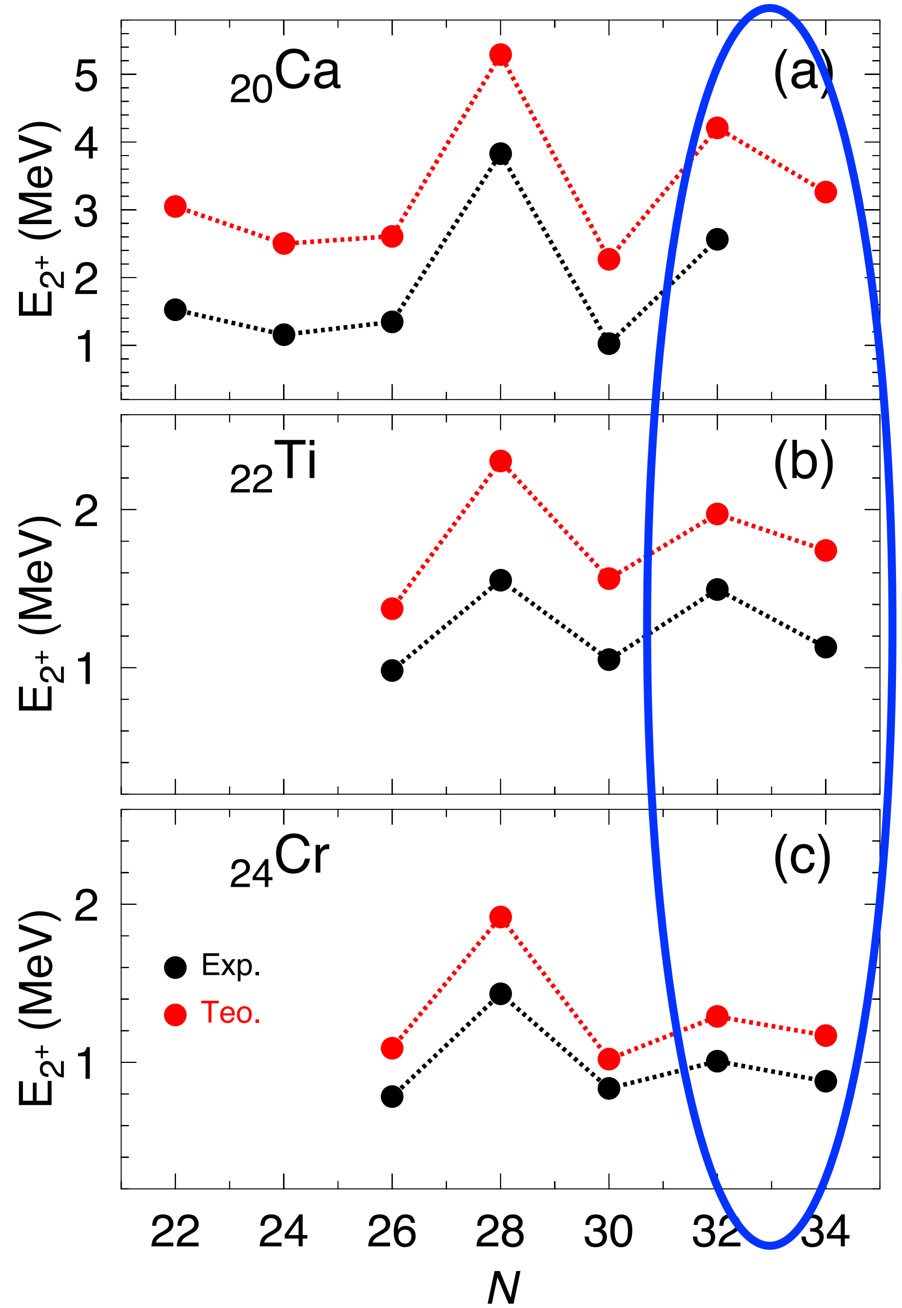

✓ AXIAL calculations

✓ Good agreement in the binding energies and two neutron separation energies.

✓ Excellent qualitative agreement for the excitation energies $E(2^+)$

✓ *N*=32 is a good sub-shell closure while *N*=34 is not.

T.R.R and J.L. Egido, Phys. Rev. Lett. 99, 06201 (2007)

Shell closures

- N=32 and/or N=34 in Ca, Ti and Cr isotopes.

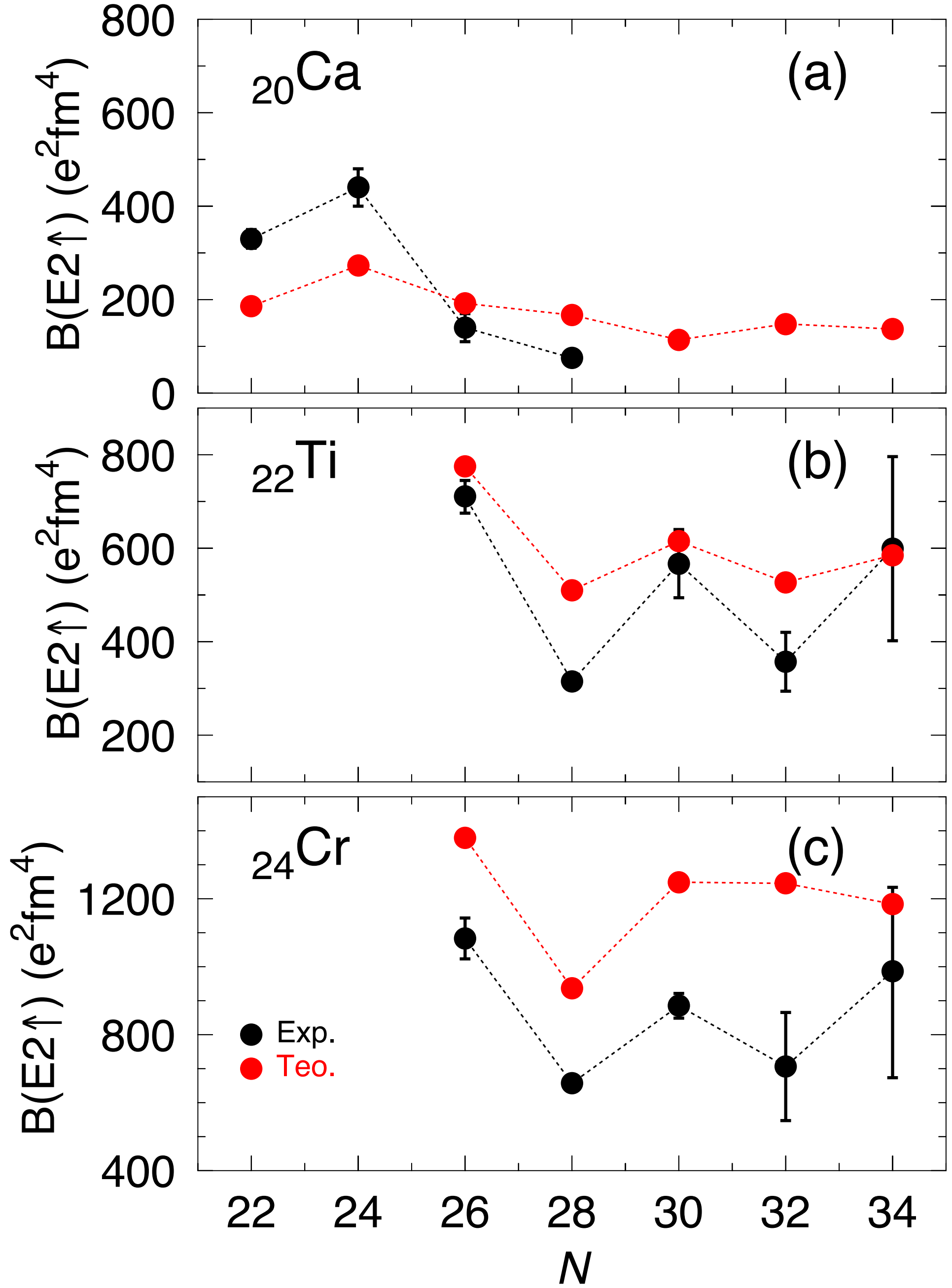

✓ AXIAL calculations

✓ Good agreement in the binding energies and two neutron separation energies.

✓ Excellent qualitative agreement for the excitation energies $E(2^+)$

✓ N=32 is a good sub-shell closure while N=34 is not.

✓ Staggering of the $B(E2)$ in Ti isotopes is reproduced without any effective charges

✓ Qualitative agreement in the $B(E2)$ especially in the lightest isotopes.

T.R.R and J.L. Egido, Phys. Rev. Lett. 99, 06201 (2007)

Shape evolution in the Cadmium isotopic chain

✓ Shape evolves from *N*=50 to *N*=82 magic number through prolate axially symmetric structures

✓ Highest deformation is found in mid-shell nuclei (β~0.2)

✓ Rest of calculations will assume axial symmetry

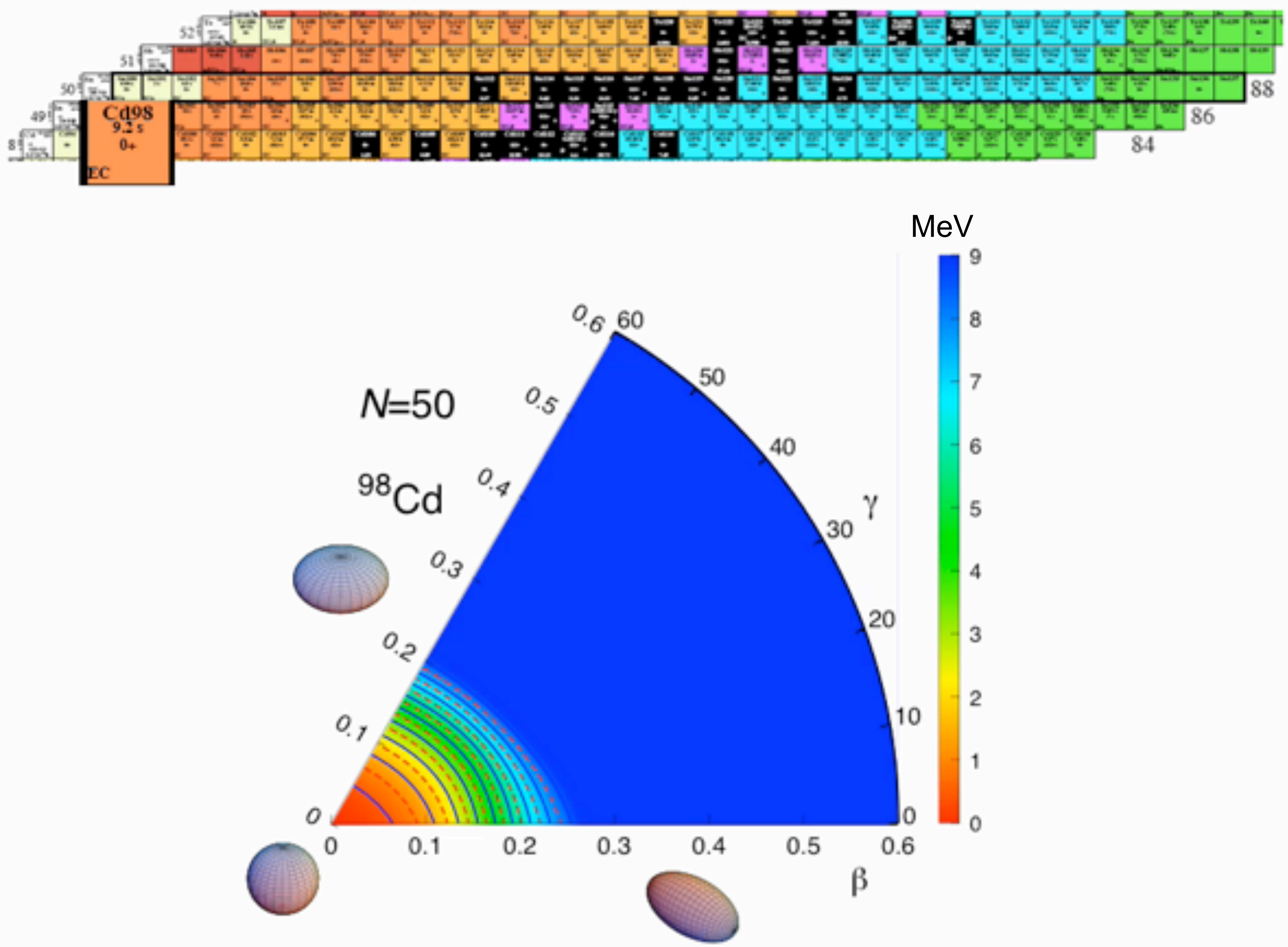

Shell closures

- Systematics of the *E*(2) and *B*(E2) in Cadmium isotopes

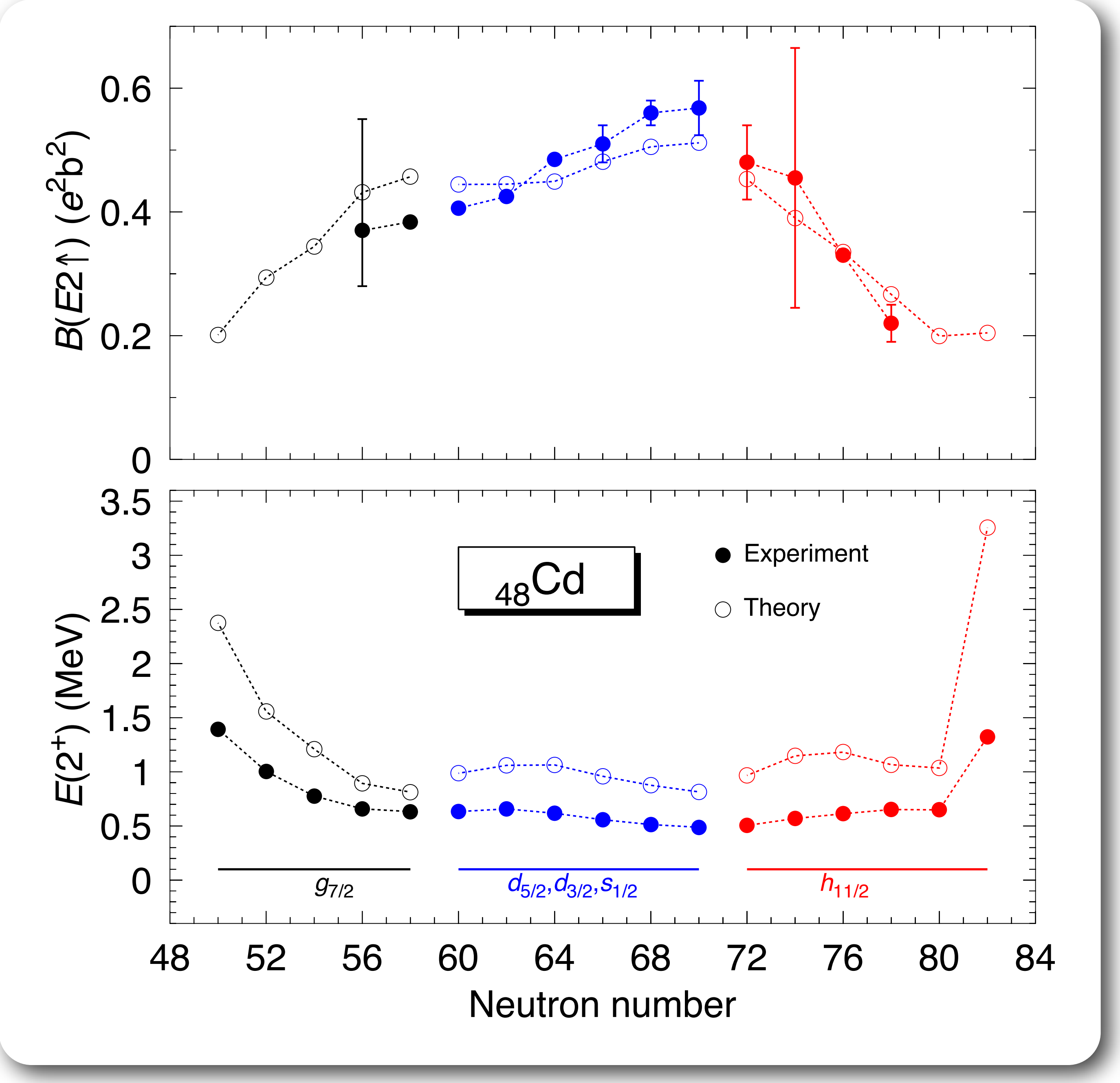

✓ AXIAL calculations

✓ Good qualitative agreement for the $E(2^+)$ excitation energies and *B*(E2) transition probabilities from shell to shell

✓ *N*=50-58 parabolic behavior (filling $g_{7/2}$ shell)

✓ *N*=60-70 flat behavior (filling $d_{5/2}$, $d_{3/2}$, $s_{1/2}$ shells)

✓ Anomalous behavior of $E(2^+)$ for ^{128}Cd has been is well reproduced

T.R.R, J.L. Egido, A. Jungclaus, Phys. Lett. B 668, 410 (2008)

Shell closures

- Systematics of the $E(2)$ and $B(E2)$ in Cadmium isotopes

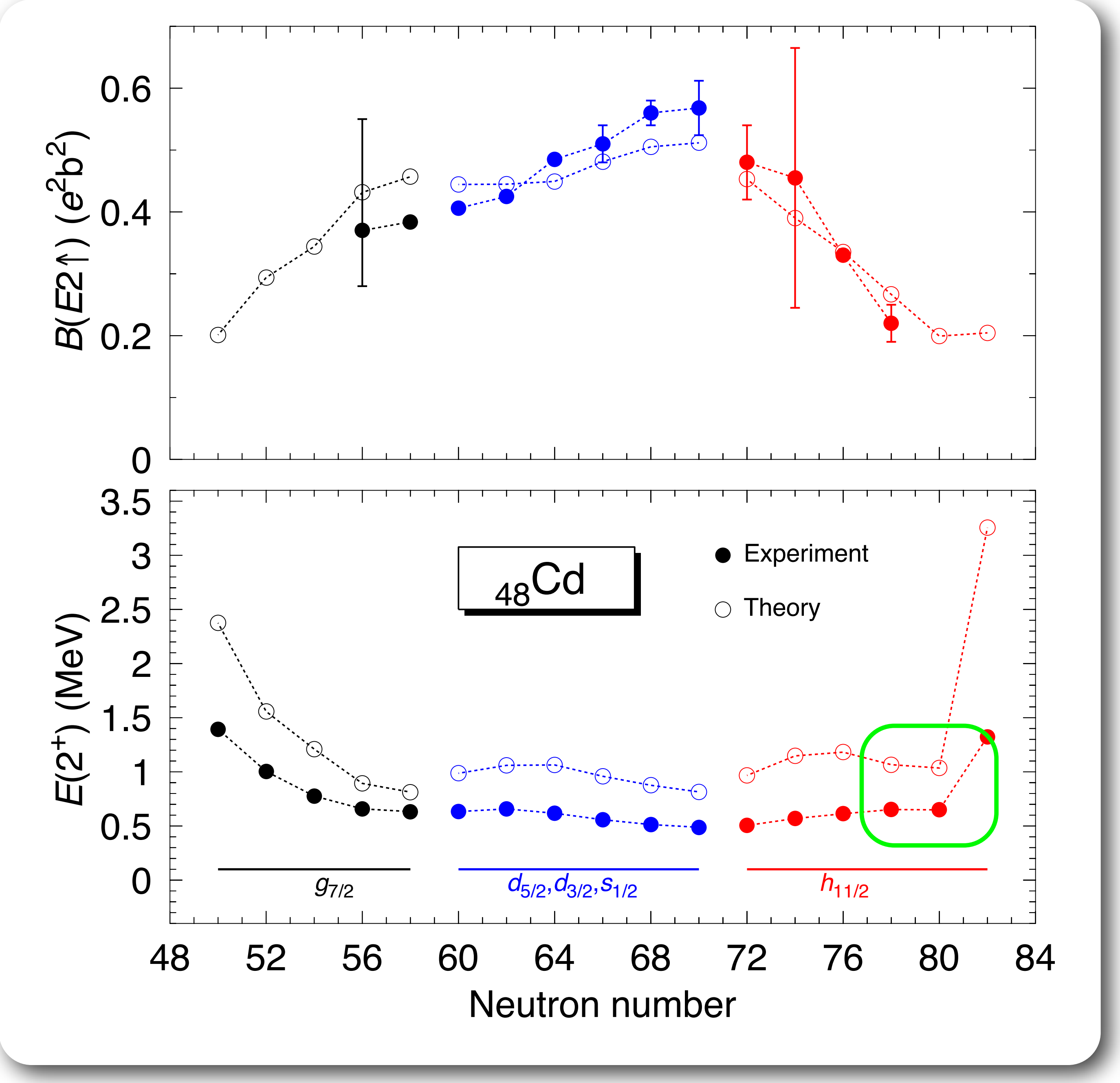

✓ AXIAL calculations

✓ Good qualitative agreement for the $E(2^+)$ excitation energies and B(E2) transition probabilities from shell to shell

✓ N=50-58 parabolic behavior (filling $g_{7/2}$ shell)

✓ N=60-70 flat behavior (filling $d_{5/2}$, $d_{3/2}$, $s_{1/2}$ shells)

✓ Anomalous behavior of $E(2^+)$ for ^{128}Cd has been is well reproduced

T.R.R, J.L. Egido, A. Jungclaus, Phys. Lett. B 668, 410 (2008)

Triaxial calculations in rp-process waiting point ^{80}Zr

- Five minima are closer in energy whenever the rotational invariance is restored.
- Absolute minima corresponds to deformed configuration β~0.55
- Barriers between the minima are less than 1 MeV. Mixing?

T.R.R and J.L. Egido, Phys. Lett. B 705, 255 (2011).

Triaxial calculations in rp-process waiting point ^{80}Zr

- Five minima are closer in energy whenever the rotational invariance is restored.
- Absolute minima corresponds to deformed configuration β~0.55
- Barriers between the minima are less than 1 MeV. Mixing?

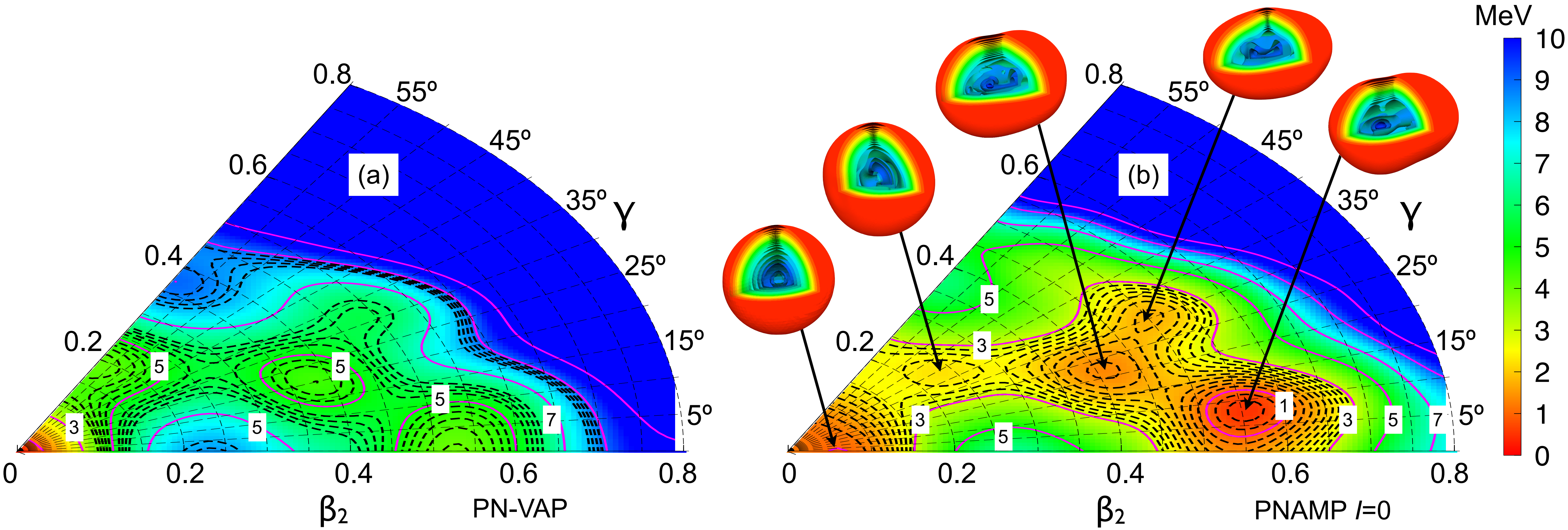

T.R.R and J.L. Egido, Phys. Lett. B 705, 255 (2011).

Triaxial calculations in rp-process waiting point ^{80}Zr

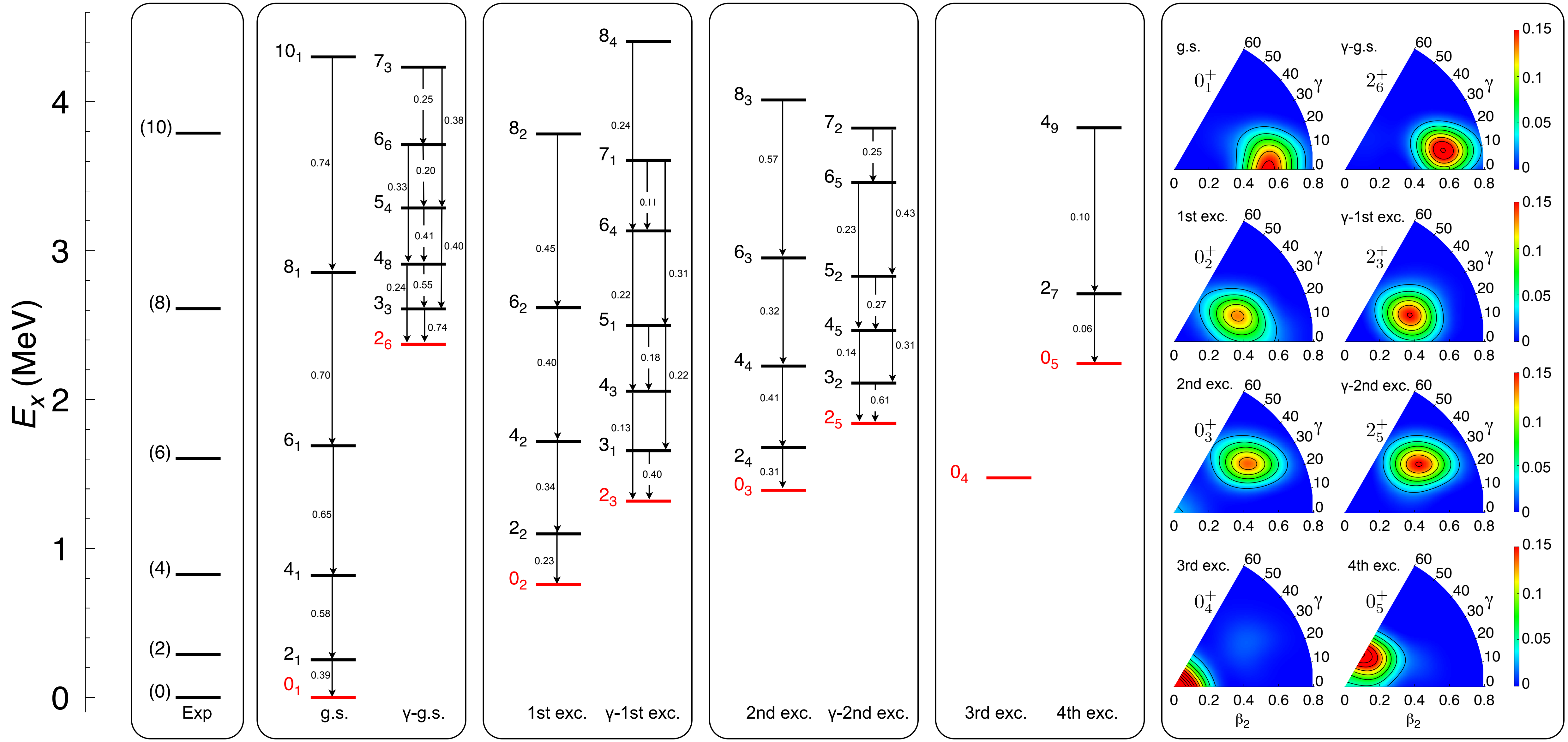

T.R.R and J.L. Egido, Phys. Lett. B 705, 255 (2011).

Triaxial calculations in rp-process waiting point ^{80}Zr

-Several rotational bands and gamma bands partners associated to the different minima of the potential energy surfaces.

- Axial ground state rotational band in agreement with the experimental levels (relevance of beyond-mean-field effects).

- Two triaxial rotational bands.

- Four excited 0^+ minima within a range of ~2.25 MeV ⇒ MULTIPLE SHAPE COEXISTENCE

- However, these levels are not thermally populated in astrophysical conditions (T~100 keV)

- Electromagnetic transitions are much faster than beta decay half-lives ⇒ NO INFLUENCE in the rp process nucleosynthesis

T.R.R and J.L. Egido, Phys. Lett. B 705, 255 (2011).

Triaxial calculations ^{44}S

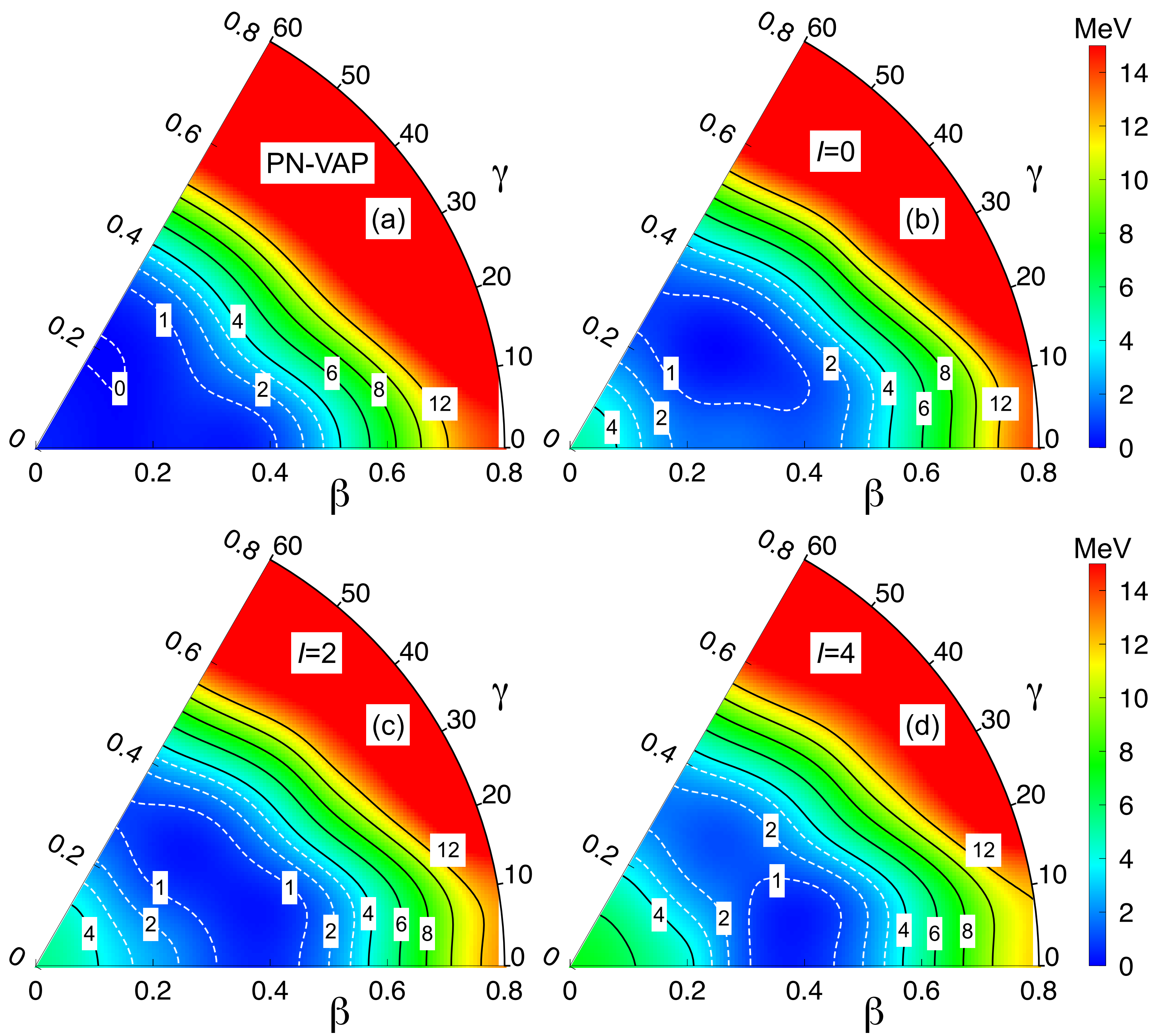

✓ *N*=28 shell closure is already broken at the PN-VAP level

✓ Very flat surface in the gamma direction: Shape mixing rather than shape coexistence

✓ Oblate shapes are a bit lower in energy for *I*=0 and the contrary for *I*=4

T.R.R and J.L. Egido, PRC 84, 051307 (2011)

Triaxial calculations ^{44}S

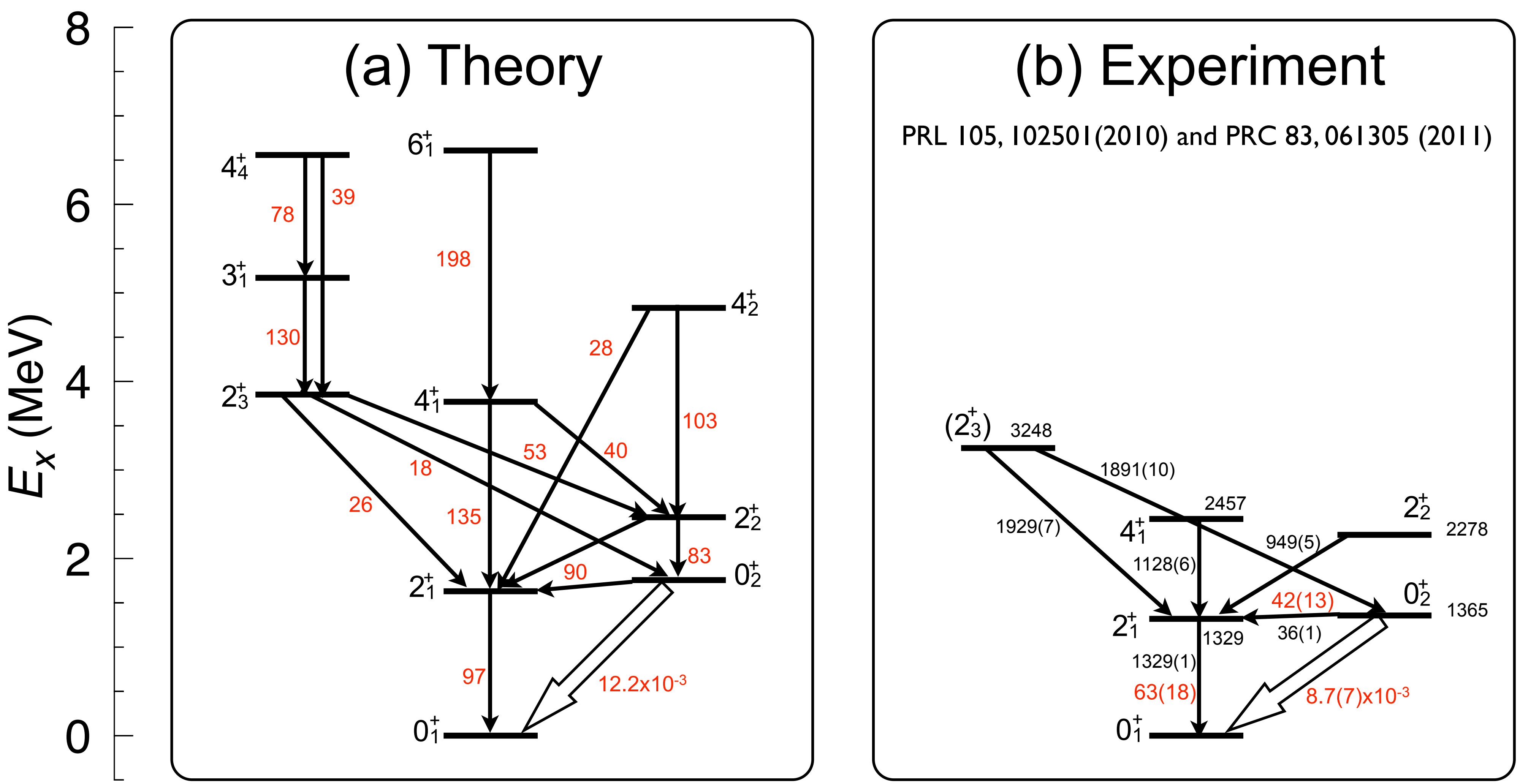

✓ Very good qualitative description of the observed levels and reduced transition probabilities.

✓ We predict three different bands strongly mixed, being the level 2^+_3 the band head of a quasi-gamma band.

T.R.R and J.L. Egido, PRC 84, 051307 (2011)

Shape mixing and coexistence

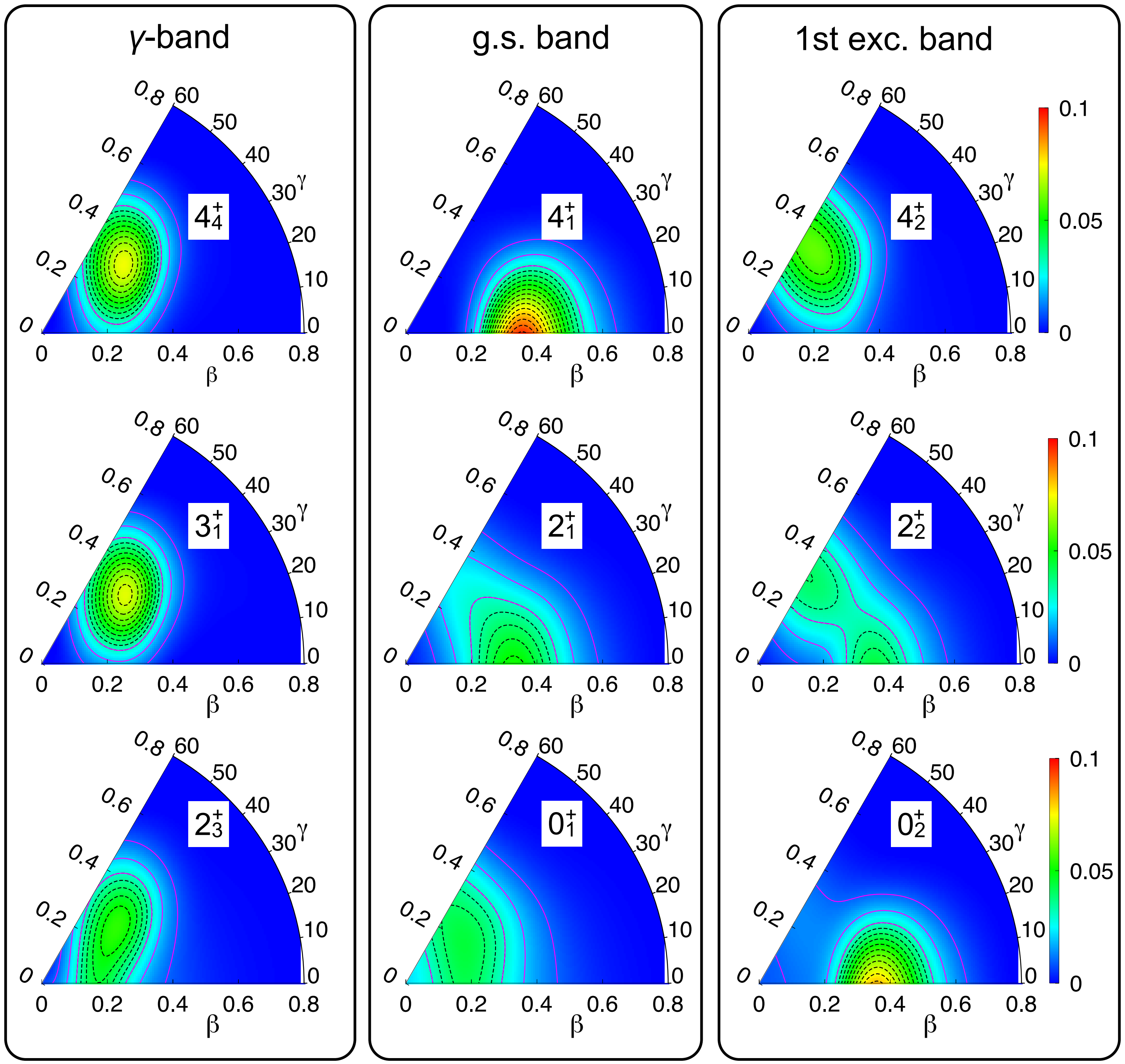

✓ Deformed ground state with triaxial shape mixing. Weakening of the *N*=28 magic number.

✓ Prolate first 0^+ excited state.

✓ There is not a clear signature of rotational structures except for the quasi-gamma band.

✓ We find shape-mixing rather shape coexistence.

T.R.R and J.L. Egido, PRC 84, 051307 (2011)

Double beta decay

Process mediated by the weak interaction which occurs in those even-even nuclei where the single beta decay is energetically forbidden.

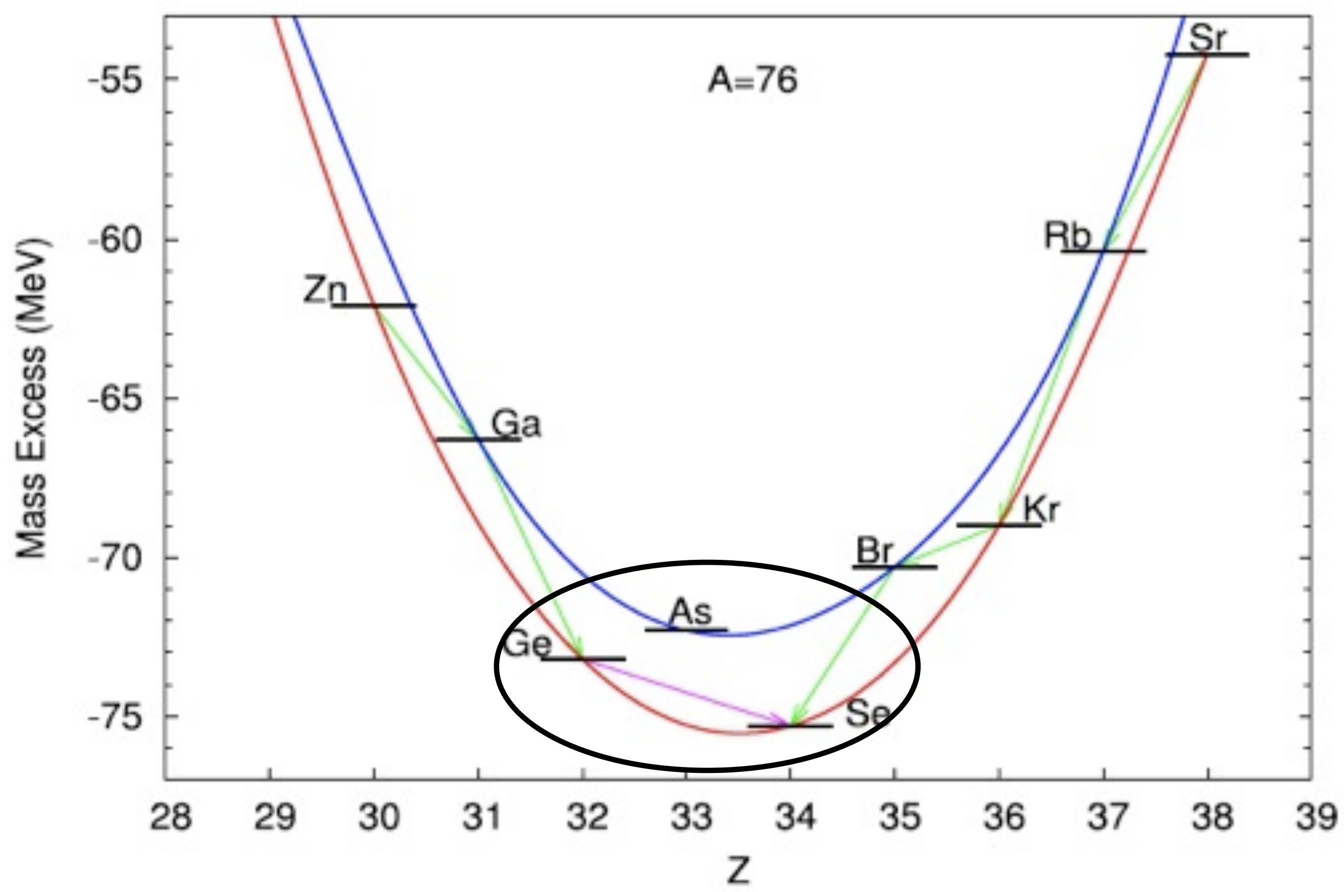

Process mediated by the weak interaction which occurs in those even-even nuclei where t... energetically forbidden.

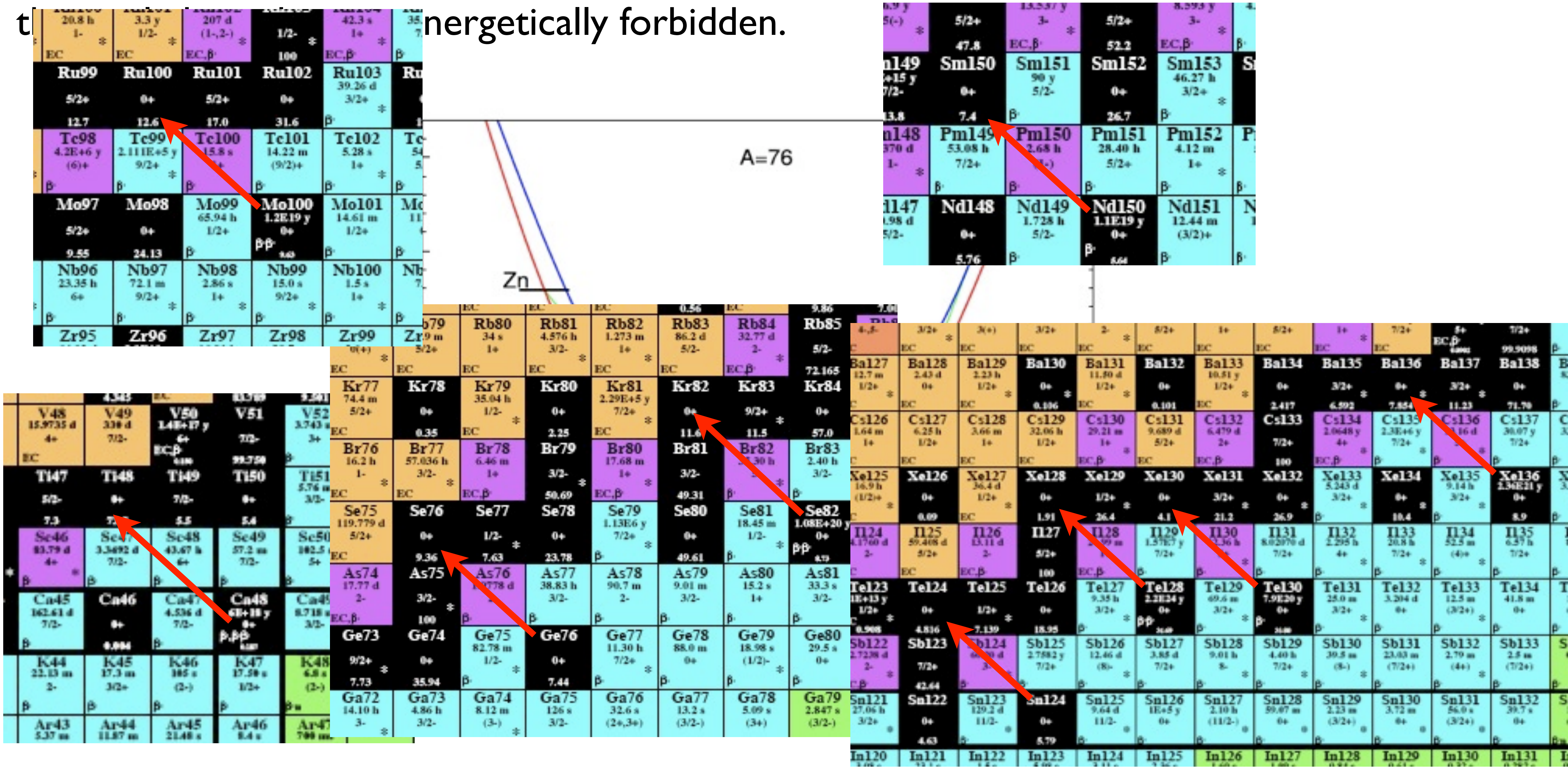

Half-life neutrinoless double beta decay (Doi et al (1985))

$$\left(T_{1/2}^{0\nu\beta\beta}(0^+ \rightarrow 0^+)\right)^{-1} = G_{01}\left|M^{0\nu\beta\beta}\right|^2\left(\frac{\langle m_\nu\rangle}{m_e}\right)^2$$

light-neutrino exchange mechanism

- Kinematic phase space factor:

$$G_{01} = \frac{(Gg_A(0))^4 m_e^4}{64\pi^5 \ln 2}\int F_0(Z,\varepsilon_1)F_0(Z,\varepsilon_2)$$
$$\times p_1 p_2 \delta(\varepsilon_1 + \varepsilon_2 - E_f - E_i)d\varepsilon_1 d\varepsilon_2 d(\hat{\vec{p}}_1 \cdot \hat{\vec{p}}_1)$$

- Effective neutrino mass:

$$\langle m_\nu\rangle = \sum_j U_{ej}^2 m_j$$

- Nuclear Matrix Element (NME):

$$M^{0\nu\beta\beta} = -\left(\frac{g_V(0)}{g_A(0)}\right)^2 M_F^{0\nu\beta\beta} + M_{GT}^{0\nu\beta\beta} - M_T^{0\nu\beta\beta}$$

Fermi Gamow-Teller Tensor

Nuclear Matrix Elements

TECHNISCHE UNIVERSITÄT DARMSTADT

$$M^{0\nu\beta\beta}=-\left(\frac{g_V(0)}{g_A(0)}\right)^2 M_F^{0\nu\beta\beta}+M_{GT}^{0\nu\beta\beta}-M_T^{0\nu\beta\beta}$$

- Each term can be written as the expectation value of a transition operator acting on the initial al final states:

$$M_\xi^{0\nu\beta\beta}=\langle 0_f^+|\hat{O}_\xi^{0\nu\beta\beta}|0_i^+\rangle$$

- Nuclear structure methods for calculating these NME:
  - Quasiparticle Random Phase Approximation in different versions: QRPA, RQRPA, SRQRPA. (Tübingen group, Jyüvaskylä group)
  - Interacting Shell Model -ISM- (Strasbourg-Madrid collaboration, Michigan)
  - Interacting Boson Model -IBM- (Yale group)
  - Projected Hartree-Fock-Bogoliubov -PHFB- (Lucknow-UNAM group)
  - Energy Density Functional

Nuclear Matrix Elements

$$M^{0\nu\beta\beta}=-\left(\frac{g_V(0)}{g_A(0)}\right)^2 M_F^{0\nu\beta\beta}+M_{GT}^{0\nu\beta\beta}-M_T^{0\nu\beta\beta}$$

- Each term can be written as the expectation value of a transition operator acting on the initial al final states:

$$M_{\xi}^{0\nu\beta\beta}=\langle 0_f^+|\hat{O}_{\xi}^{0\nu\beta\beta}|0_i^+\rangle$$

- Nuclear structure methods for calculating these NME:

Different ways to deal with:
- Finding the best initial and final ground states.
- Handling the transition operator (inclusion of most relevant terms, corrections, approximations, etc.).

Some remarks about these methods:
- Calculations with limited single particle bases.
- Interactions fitted to the specific region (ISM) or to each nucleus individually (rest).
- Difficulties to include collective degrees of freedom.
- Problems with particle number conservation.

$$\frac{\langle 0; N_f Z_f; q_f | \hat{O}_{\xi}^{0\nu\beta\beta} | 0; N_i Z_i; q_i \rangle}{\sqrt{\langle 0; N_f Z_f; q_f | 0; N_f Z_f; q_f \rangle \langle 0; N_i Z_i; q_i | 0; N_i Z_i; q_i \rangle}}$$

A=150

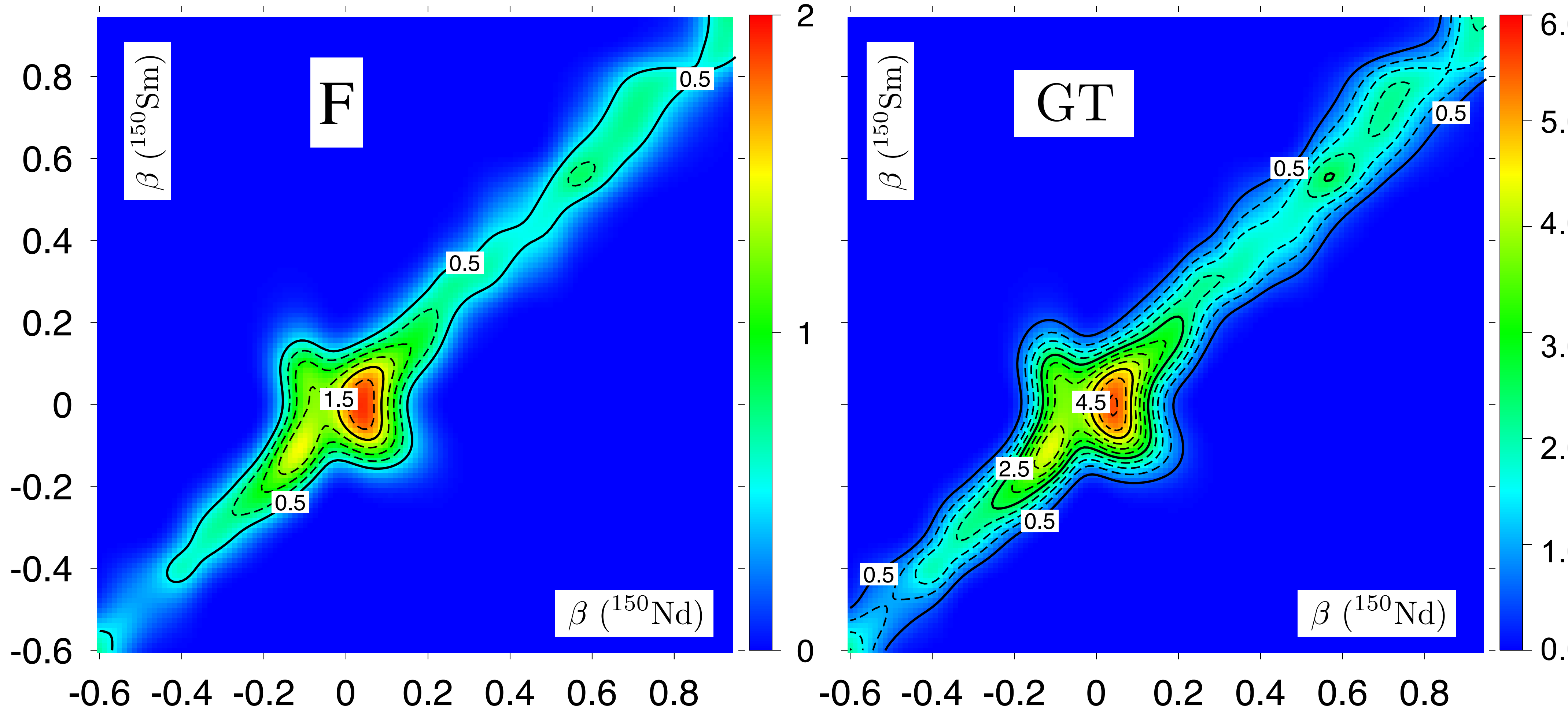

- GT strength greater than Fermi.
- Similar deformation between mother and granddaughter is favored by the transition operators
- Maxima are found close to sphericity although some other local maxima are found

NME: deformation and mixing

$$\frac{\langle 0; N_f Z_f; q_f | \hat{O}_{\xi}^{0\nu\beta\beta} | 0; N_i Z_i; q_i \rangle}{\sqrt{\langle 0; N_f Z_f; q_f | 0; N_f Z_f; q_f \rangle \langle 0; N_i Z_i; q_i | 0; N_i Z_i; q_i \rangle}}$$

A=150

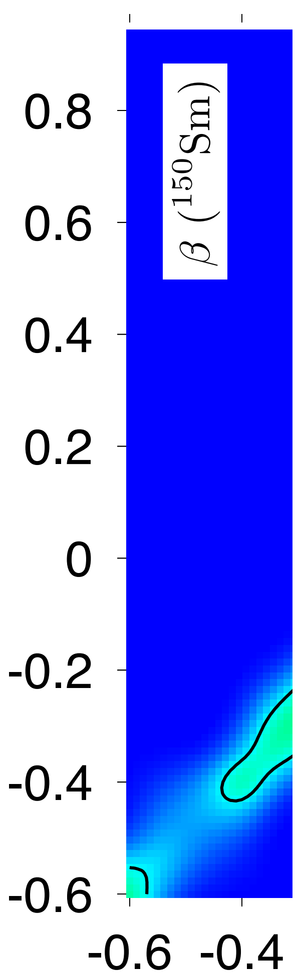

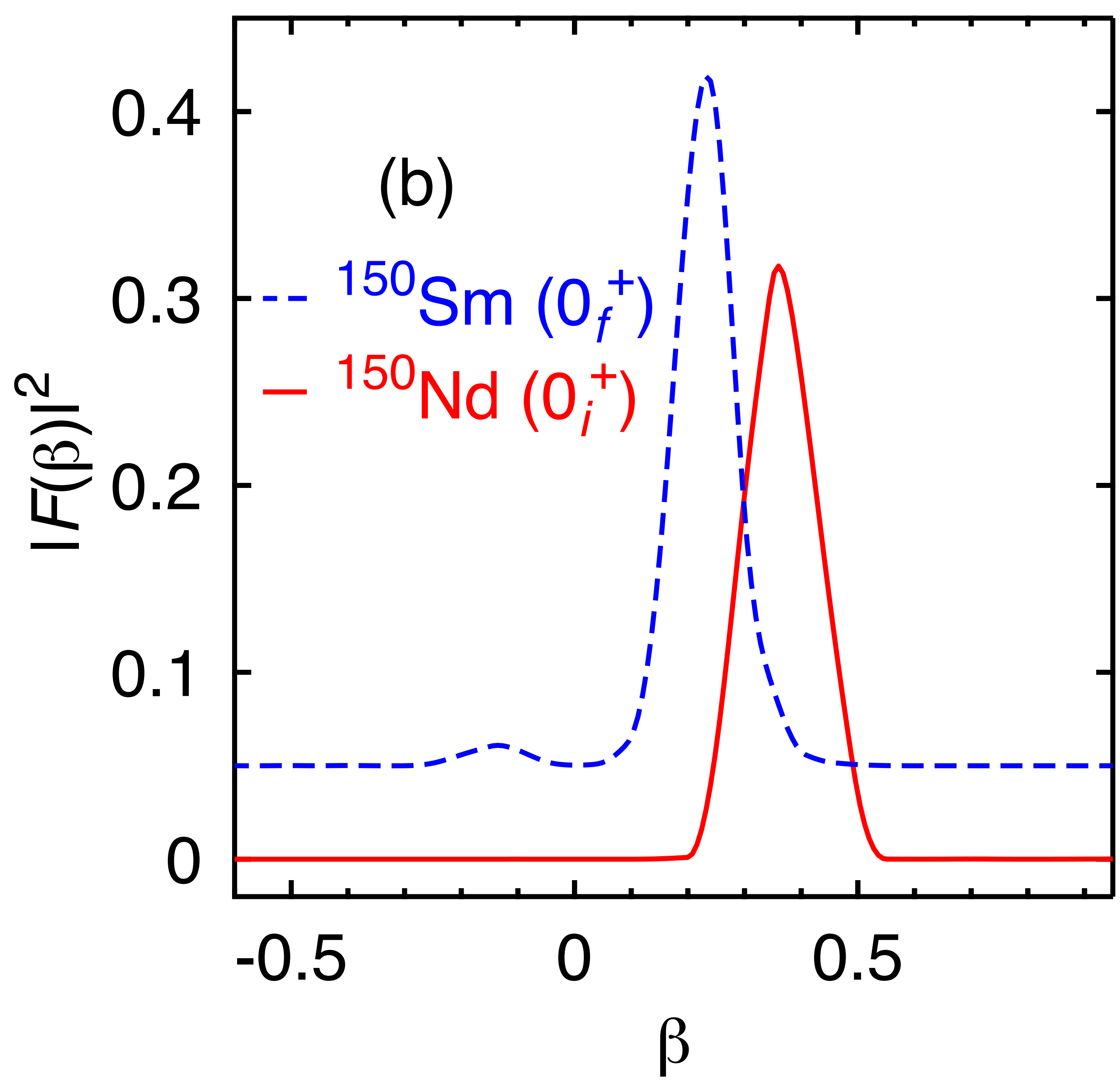

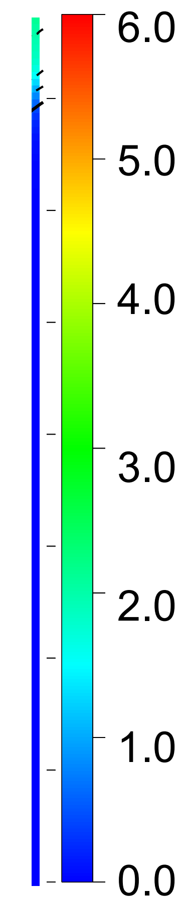

- GT stren ... rs
- Similar de
- Maxima a
- Final resu ... llective states with... this plot

NME: deformation and mixing

$$\frac{\langle 0; N_f Z_f; q_f | \hat{O}^{0\nu\beta\beta}_{\xi} | 0; N_i Z_i; q_i \rangle}{\sqrt{\langle 0; N_f Z_f; q_f | 0; N_f Z_f; q_f \rangle \langle 0; N_i Z_i; q_i | 0; N_i Z_i; q_i \rangle}}$$

A=150

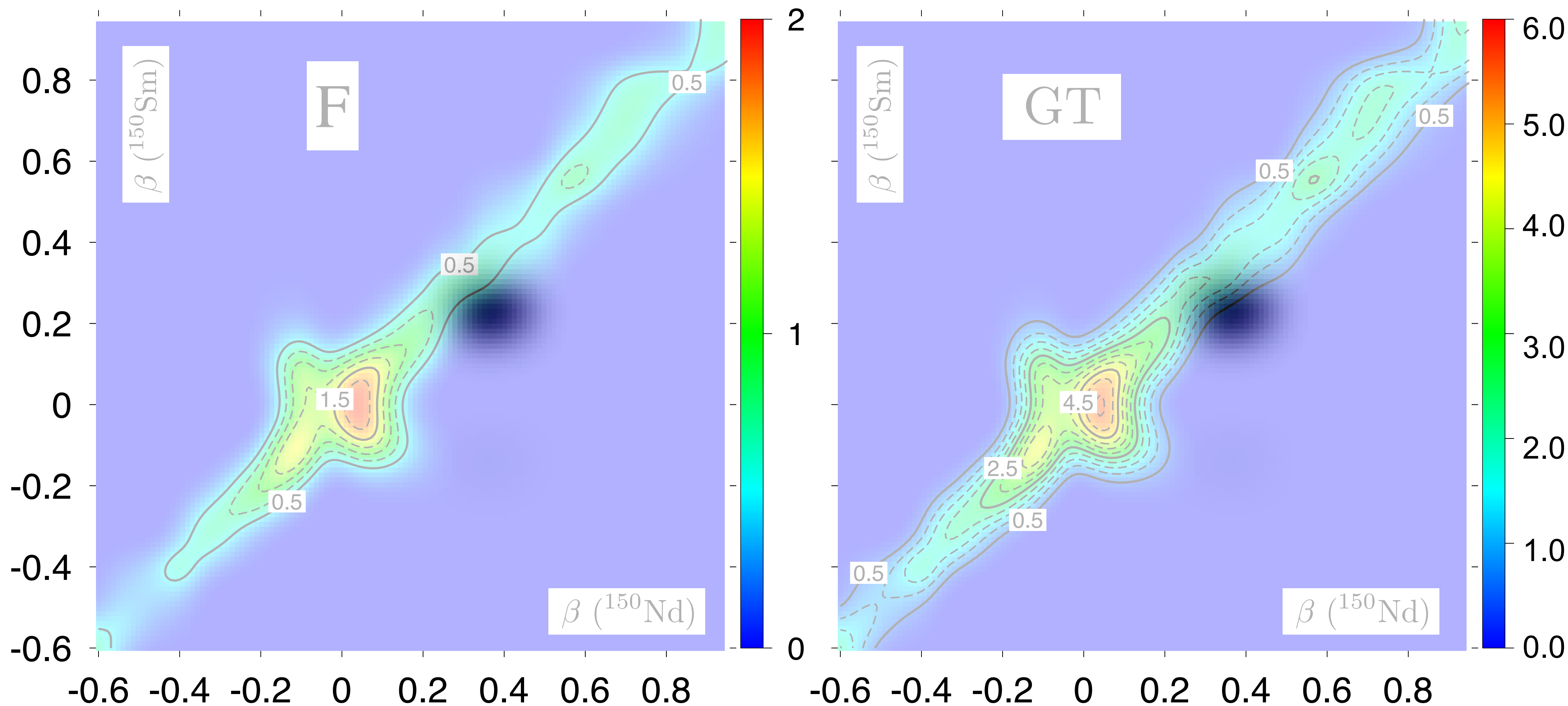

- GT strength greater than Fermi.
- Similar deformation between mother and granddaughter is favored by the transition operators
- Maxima are found close to sphericity although some other local maxima are found
- Final result depends on the distribution of probability of the corresponding initial and final collective states within this plot

NME: deformation and mixing

$$\frac{\langle 0; N_fZ_f; q_f|\hat{O}_{\xi}^{0\nu\beta\beta}|0; N_iZ_i; q_i\rangle}{\sqrt{\langle 0; N_fZ_f; q_f|0; N_fZ_f; q_f\rangle\langle 0; N_iZ_i; q_i|0; N_iZ_i; q_i\rangle}}$$

A=150

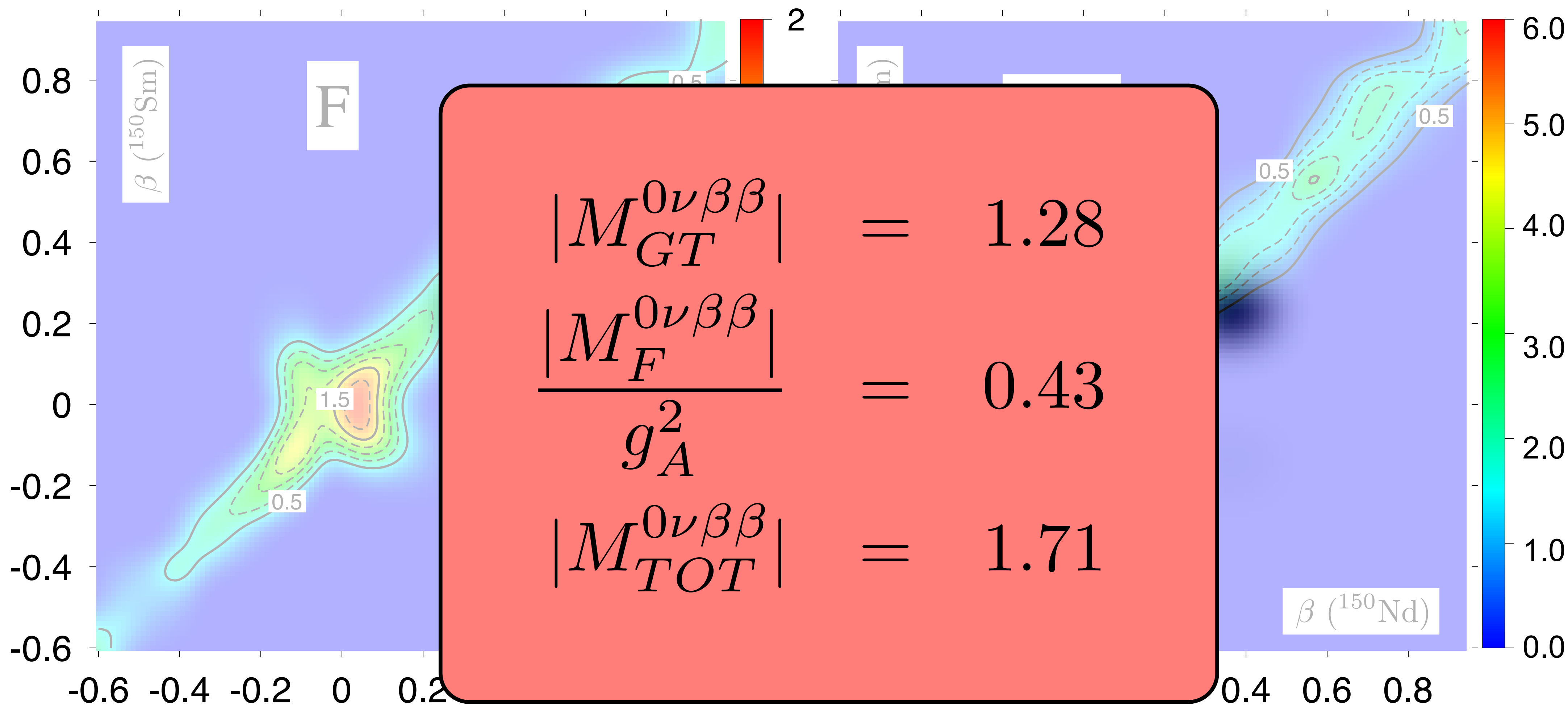

$$|M^{0\nu\beta\beta}_{GT}| = 1.28$$

$$\frac{|M^{0\nu\beta\beta}_{F}|}{g_A^2} = 0.43$$

$$|M^{0\nu\beta\beta}_{TOT}| = 1.71$$

- GT strength greater than Fermi.
- Similar deformation between mother and granddaughter is favored by the transition operators
- Maxima are found close to sphericity although some other local maxima are found
- Final result depends on the distribution of probability of the corresponding initial and final collective states within this plot

NME: deformation and mixing

$$\frac{\langle 0; N_f Z_f; q_f|\hat{O}^{0\nu\beta\beta}_{\xi}|0; N_i Z_i; q_i\rangle}{\sqrt{\langle 0; N_f Z_f; q_f|0; N_f Z_f; q_f\rangle\langle 0; N_i Z_i; q_i|0; N_i Z_i; q_i\rangle}}$$

A=76

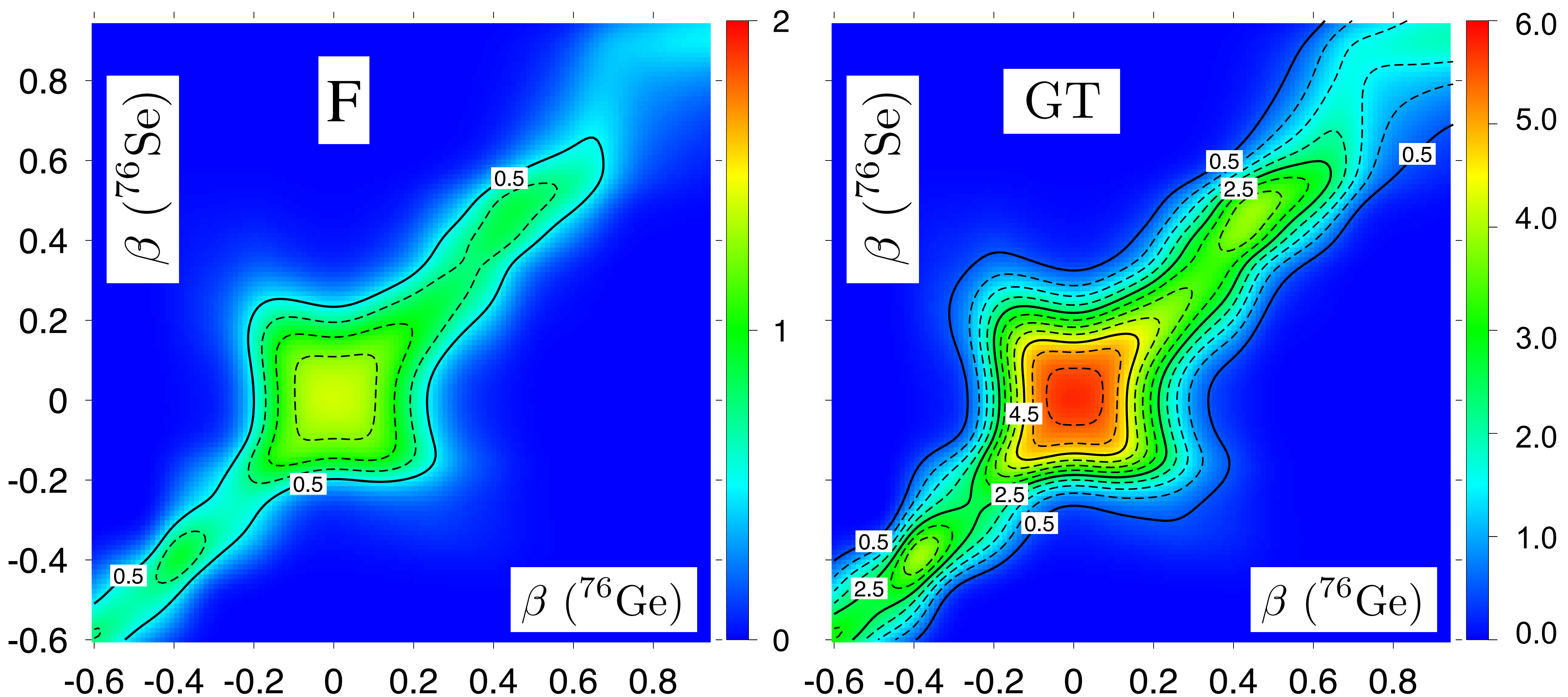

- GT strength greater than Fermi.
- Similar deformation between mother and granddaughter is favored by the transition operators
- Maxima are found close to sphericity although some other local maxima are found

NME: deformation and mixing

$$\frac{\langle 0;N_fZ_f;q_f|\hat{O}^{0\nu\beta\beta}_{\xi}|0;N_iZ_i;q_i\rangle}{\sqrt{\langle 0;N_fZ_f;q_f|0;N_fZ_f;q_f\rangle\langle 0;N_iZ_i;q_i|0;N_iZ_i;q_i\rangle}}$$

A=76

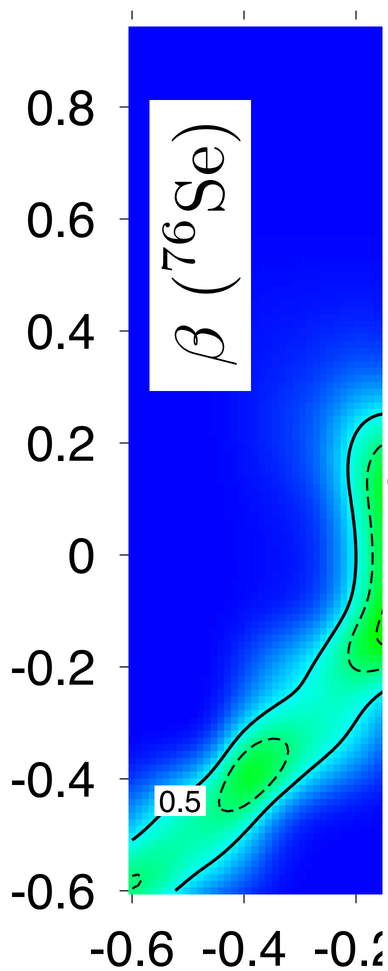

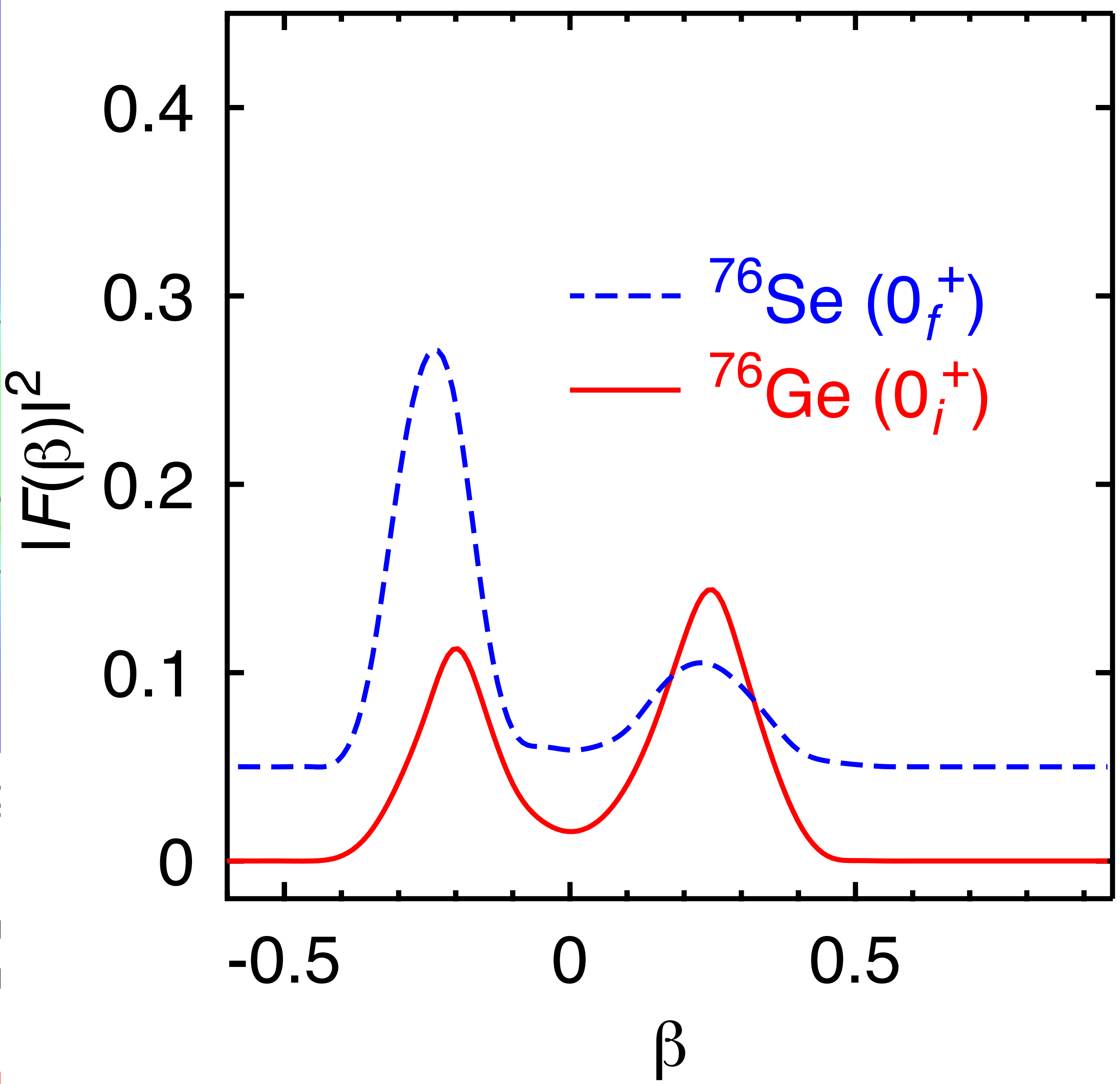

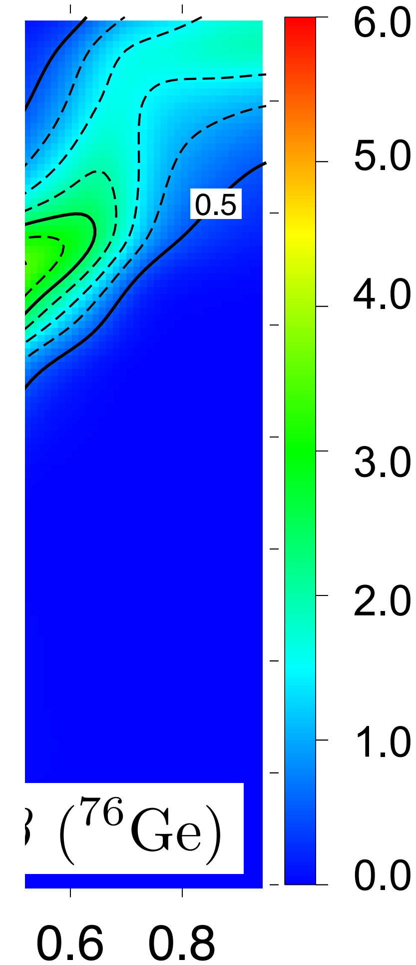

- GT strength ... ion operators
- Similar defo ... d
- Maxima are
- Final result ... and final collective states within

NME: deformation and mixing

$$\frac{\langle 0; N_f Z_f; q_f | \hat{O}_{\xi}^{0\nu\beta\beta} | 0; N_i Z_i; q_i \rangle}{\sqrt{\langle 0; N_f Z_f; q_f | 0; N_f Z_f; q_f \rangle \langle 0; N_i Z_i; q_i | 0; N_i Z_i; q_i \rangle}}$$

A=76

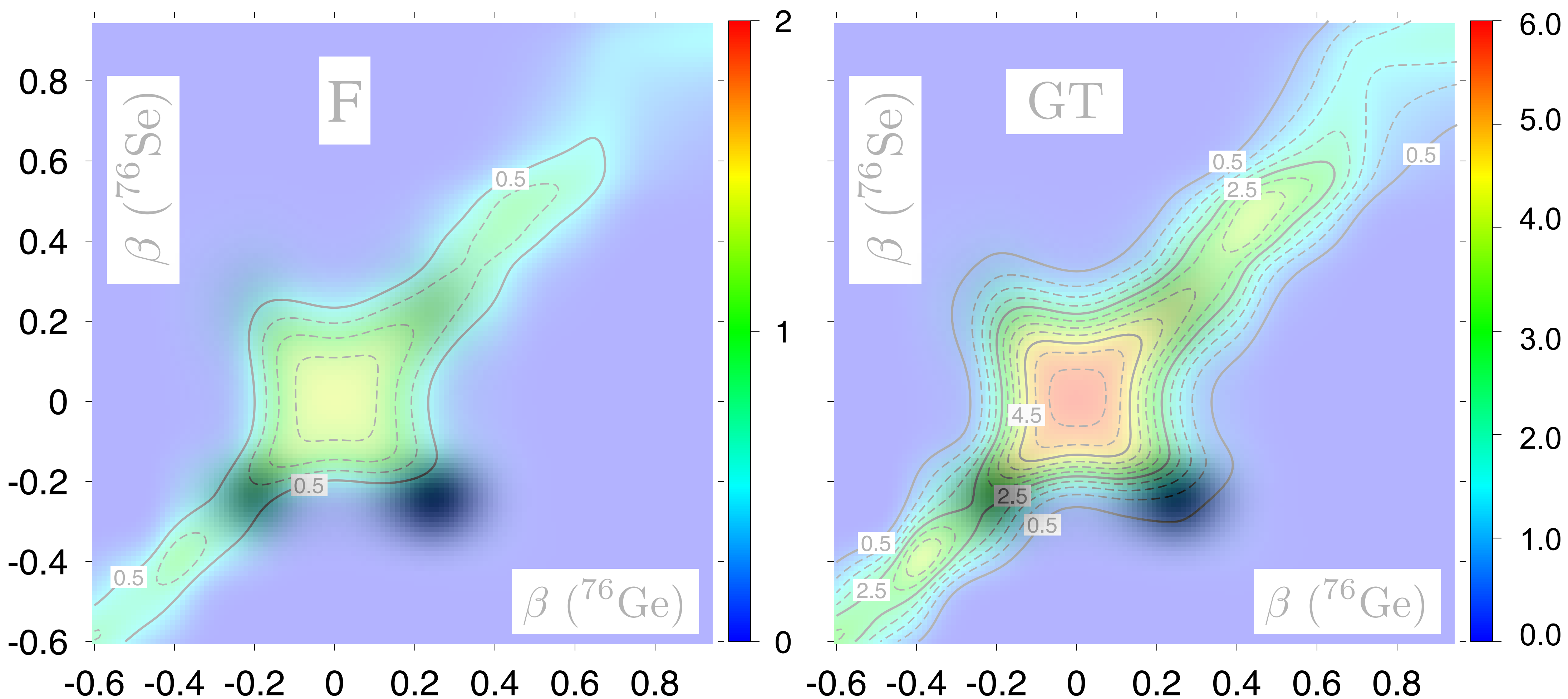

- GT strength greater than Fermi.
- Similar deformation between mother and granddaughter is favored by the transition operators
- Maxima are found close to sphericity although some other local maxima are found
- Final result depends on the distribution of probability of the corresponding initial and final collective states within this plot

NME: deformation and mixing

$$\frac{\langle 0; N_f Z_f; q_f | \hat{O}_{\xi}^{0\nu\beta\beta} | 0; N_i Z_i; q_i \rangle}{\sqrt{\langle 0; N_f Z_f; q_f | 0; N_f Z_f; q_f \rangle \langle 0; N_i Z_i; q_i | 0; N_i Z_i; q_i \rangle}}$$

A=76

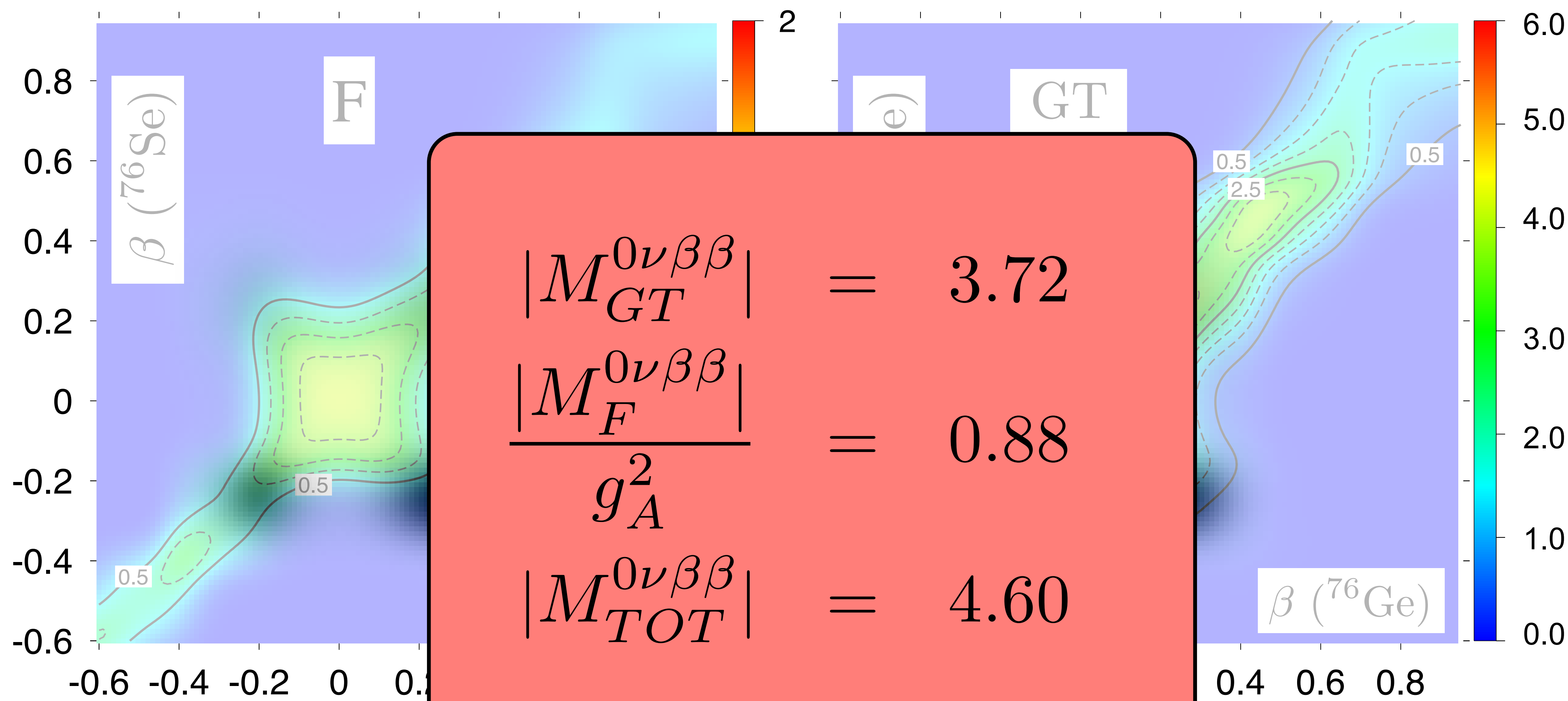

$$|M_{GT}^{0\nu\beta\beta}| = 3.72$$

$$\frac{|M_{F}^{0\nu\beta\beta}|}{g_A^2} = 0.88$$

$$|M_{TOT}^{0\nu\beta\beta}| = 4.60$$

- GT strength greater than Fermi.
- Similar deformation between mother and granddaughter is favored by the transition operators
- Maxima are found close to sphericity although some other local maxima are found
- Final result depends on the distribution of probability of the corresponding initial and final collective states within this plot

NME: deformation and mixing

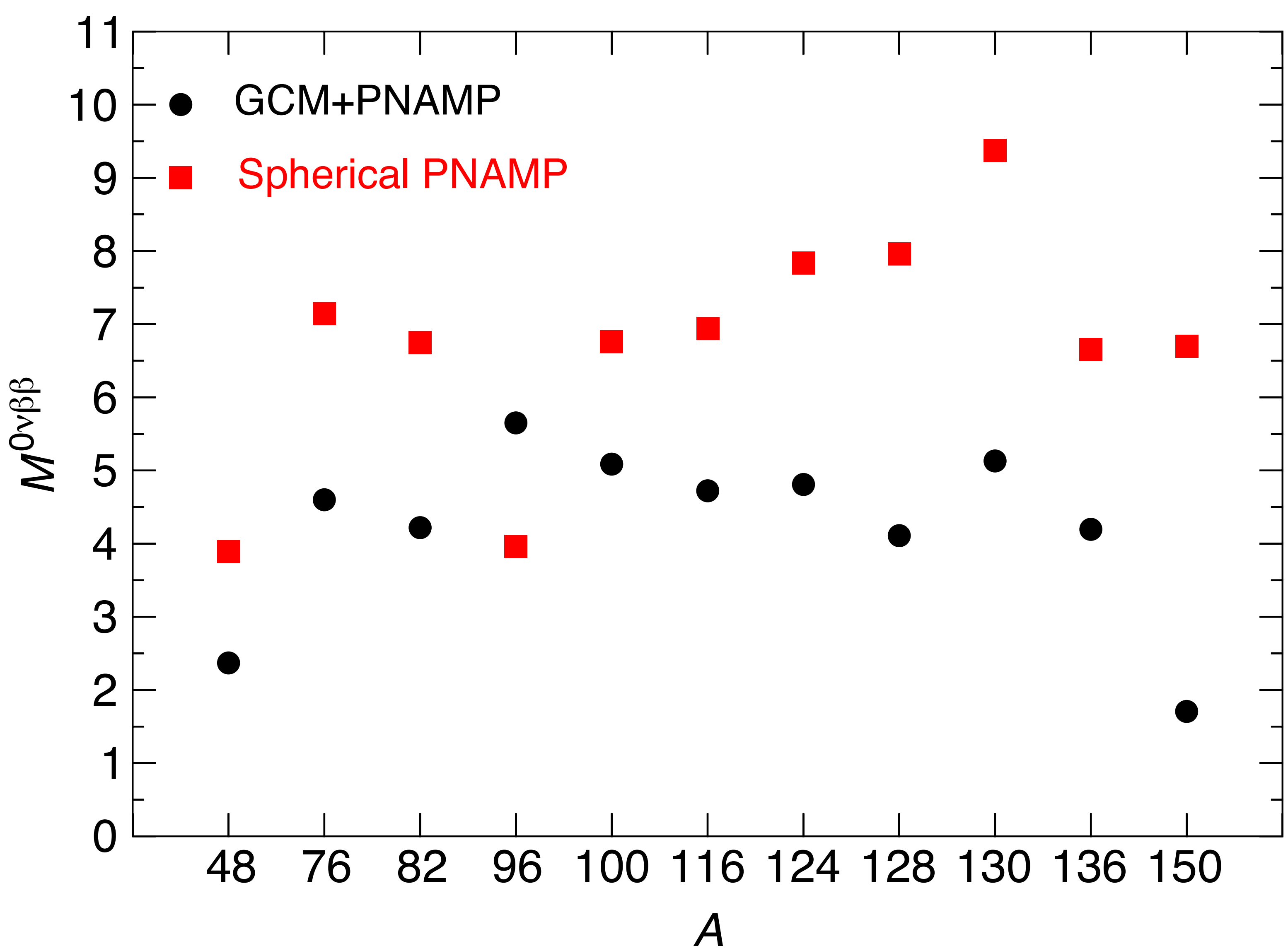

Noticeable difference in the NME if only intrinsic spherical configurations are considered without configuration mixing.

NME: Summary of the results

TECHNISCHE UNIVERSITÄT DARMSTADT

Gogny D1S parametrization

A	48	76	82	96	100	116	124	128	130	136	150	152	164	180
$M^{0\nu}$	2.37	4.60	4.22	5.65	5.08	4.72	4.81	4.11	5.13	4.20	1.71	1.07	0.64	0.58
$T_{1/2}$ (y)	28.5 $\times10^{23}$	76.9 $\times10^{23}$	20.8 $\times10^{23}$	5.48 $\times10^{23}$	8.64 $\times10^{23}$	9.24 $\times10^{23}$	16.2 $\times10^{23}$	343.1 $\times10^{23}$	8.84 $\times10^{23}$	12.7 $\times10^{23}$	16.5 $\times10^{23}$	4.2 $\times10^{31}$	1.3 $\times10^{36}$	1.6 $\times10^{34}$

Gogny D1M parametrization

A	48	76	82	96	100	116	124	128	130	136	150	152	164	180
$M^{0\nu}$	2.43	4.64	4.28	5.70	5.19	4.83	4.71	3.98	5.07	4.29	1.36	0.89	0.50	0.38
$T_{1/2}$ (y)	27.1 $\times10^{23}$	75.6 $\times10^{23}$	20.2 $\times10^{23}$	5.38 $\times10^{23}$	8.28 $\times10^{23}$	8.82 $\times10^{23}$	16.9 $\times10^{23}$	365.8 $\times10^{23}$	9.05 $\times10^{23}$	12.2 $\times10^{23}$	26.1 $\times10^{23}$	6.2 $\times10^{31}$	2.1 $\times10^{36}$	3.8 $\times10^{34}$

double beta decay (A = 48–150) | double electron capture (A = 152–180)

NME: Summary of the results

T.R.R., Martínez-Pinedo, PRL 2010

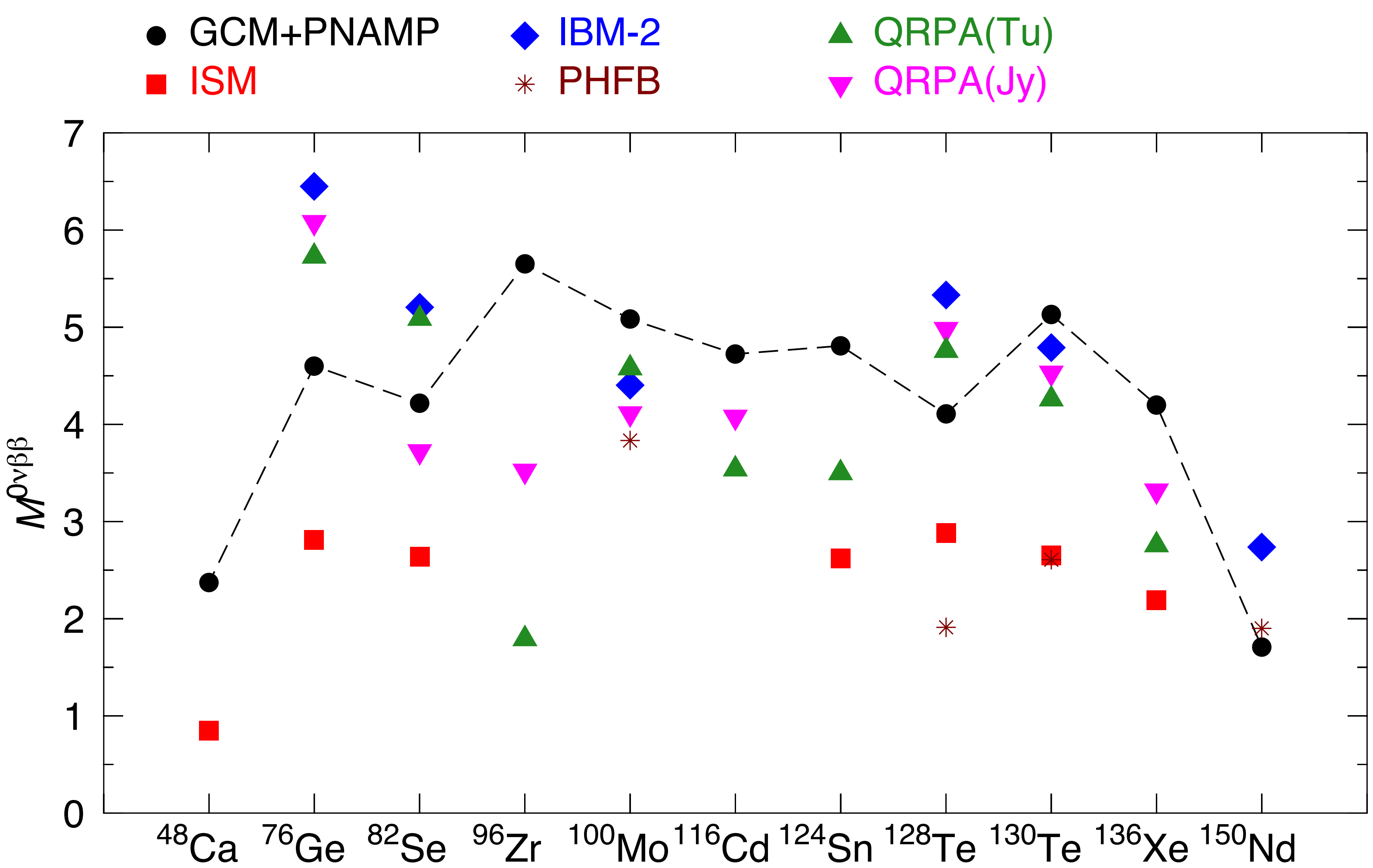

QRPA (Jy):)M. Kortelainen, J. Suhonen, PRC 75, 051303(R) (2007) and PRC 76, 024315 (2007)

QRPA(Tu): F. Simkovic et al., PRC 77, 045503 (2008)

ISM: J. Menendez et al., PRL 100, 52503 (2008)

IBM-2:J. Barea, F. Iachello, PRC 77, 045503 (2008)

PHFB: K. Chaturvedi et al. PRC 78, 054302 (2008)

- Higher values than the ones predicted by ISM calculations (larger valence space, lower seniority components).
- For *A*=76, 82, 128, 150 we predict smaller values than the ones given by QRPA and/or IBM while for *A*=96, 100, 116, 124, 130, 136 larger values are obtained.
- Consistent results with the rest of the models. Notice that we are using the same interaction for all the nuclei.
- Further studies are needed to understand what is missing in the different models.

NME: Summary of the results

T.R.R., Martínez-Pinedo, PRL 2010

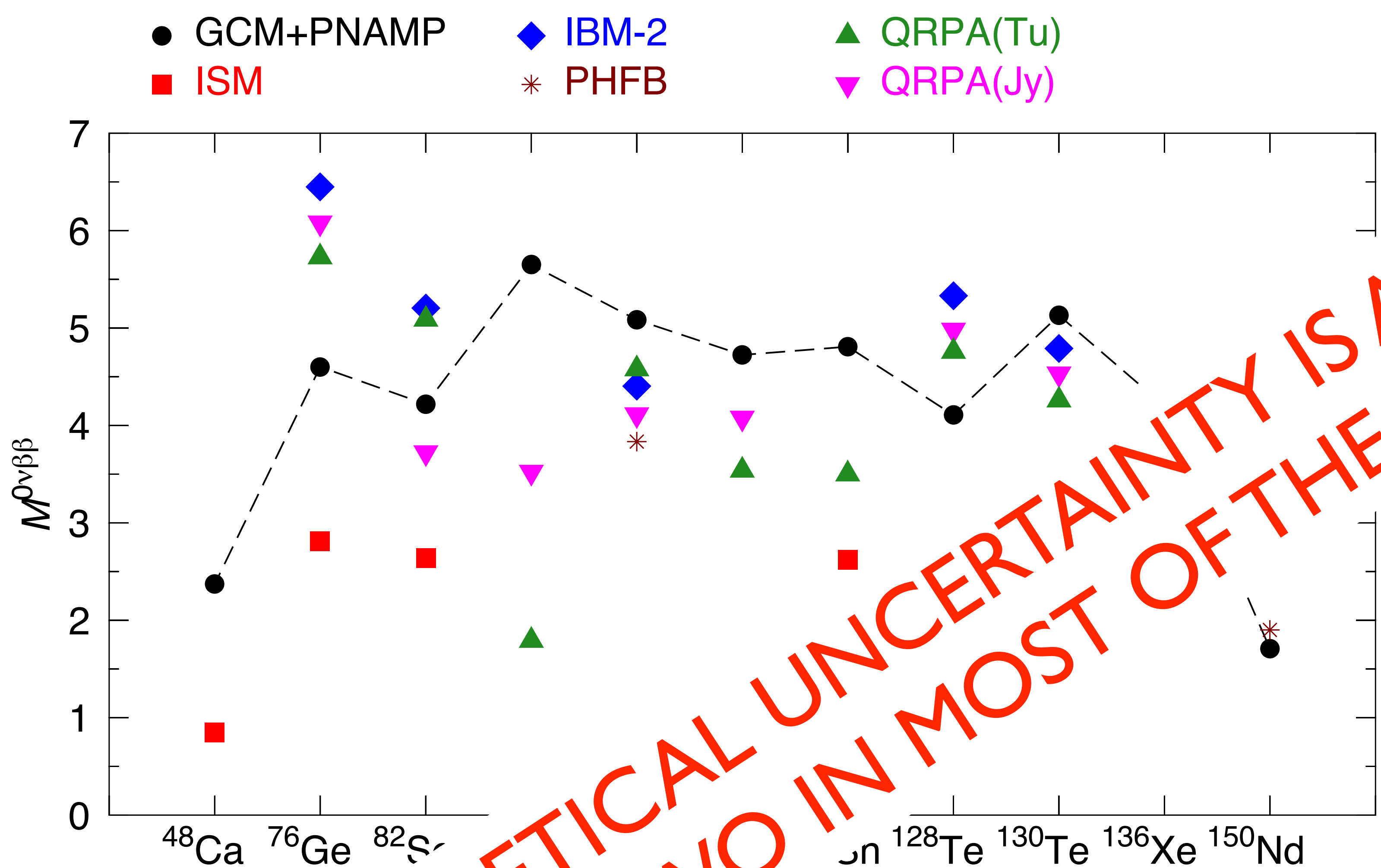

QRPA (Jy): M. Kor...en, J. Suhonen, ...51303(R) ... PRC 76, ...

... Simkovic ... PRC 77, 045503 ...

ISM: J. Menendez et al., PRL 100, 52503 (2008)

IBM-2: J. Barea, F. Iachello, PRC 77, 045503 (2008)

PHFB: K. Chaturvedi et al. PRC 78, 054302 (2008)

THEORETICAL UNCERTAINTY IS A FACTOR TWO IN MOST OF THE CASES

- Higher valu... ...ted by ISM calculations (larger valence space, lower seniority compone...
- For *A*=76... predict smaller values than the ones given by QRPA and/or IBM while for *A*=96, 10... 130, 136 larger values are obtained.
- Consistent r... with the rest of the models. Notice that we are using the same interaction for all the nuclei.
- Further studies are needed to understand what is missing in the different models.

Summary and outlook

- Energy density functional methods provide a reliable description of nuclear structure observables and NMEs in lepton number violating processes.
- Other degrees of freedom should be also explored (pairing vibrations, octupole deformations, triaxiality, explicit quasiparticle excitations...)
- Need of energy density functionals adjusted to beyond mean field results.
- Description of odd nuclei at the same level.

Acknowledgments

TECHNISCHE UNIVERSITÄT DARMSTADT

G. Martínez-Pinedo (TU-Darmstadt)
K. Langanke (GSI-Darmstadt)
J. L. Egido (UAM-Madrid)
K. Blaum (U-Heidelberg)
C. Smorra (U-Heidelberg)